Deformation and Fracture Behavior of Thermomechanical Bonds in Nonwoven Fabrics

Joseph Anderson Rittenhouse

Thesis submitted to the faculty of the Virginia Polytechnic Institute and State University in partial fulfillment of the requirements for the degree of

Master of Science
in
Materials Science and Engineering

Robert Moore, Chair
Raffaella De Vita, Co-Chair
David Dillard
Johan Foster

July 13th, 2016
Blacksburg, VA

Keywords: Nonwoven, Fabric, Fracture behavior, Polymer, Thermoplastic

Deformation and Fracture Behavior of Thermomechanical Bonds in Nonwoven Fabric

Joseph Anderson Rittenhouse

Abstract

The market for nonwoven fabrics has experienced extreme growth in recent years and is expected to double in size from 2010 to 2020. This remarkable growth can be attributed to its numerous applications, ease of manufacturing, and customizable properties such as fabric stiffness, extensibility, and composition. The lifetime of the fabric is extremely important to producers and depends strongly on its micro-mechanical properties. Previously published studies have investigated the bulk fabric properties and the constituent fiber properties. However, nothing has been done to determine the properties of individual thermo-mechanical bonds that connect the constituent fibers of the fabric together. These bonds provide the mechanical integrity of the nonwoven fabrics. This study is the first to examine individual bonds by measuring their mechanical properties via uniaxial tensile tests and by computing the basis weight and orientation of the fibers surrounding the bonds. The results demonstrate that there is a high correlation between the fiber structure around the bond and the bond mechanical properties. The amount and directions of fibers affect how the load is transmitted through the bond and distributed across the fabric. Namely, if there are a few fibers surrounding the bond, or the primary fiber direction is different from the loading direction, then the force sustained by the bond is significantly lower and the bond does not deform. Conversely, if there are many fibers in the loading direction then the bond can sustain a significantly large force and undergoes deformation. The fiber and bond deformation are also observed through microscopic

images captured during the uniaxial tensile tests. Ultimately, this research details the results for an effective method to test and analyze the mechanical integrity of thermo-mechanically bond and the lifetime of the nonwoven fabrics.

Acknowledgements

My sincerest gratitude is given to my co-advisors, Dr. Robert Moore and Dr. Raffaella De Vita, as well as my committee member Dr. David Dillard. Dr. Moore introduced me to the field of polymer analysis through fuel cell membrane creation and encouraged me to continue research into Masters. Dr. De Vita has challenged my engineering capabilities since the first day I met her and she called on me in front of the 120-person Mechanics of Deformable Bodies class. Dr. Dillard took an immediate supervisor role on my master's project and ensured the best work was completed. These mentors have made my pursuits extremely valuable; not by making the going easy but by demanding my top effort. I thank you for enforcing that "*nothing in the world is worth having or worth doing unless it means effort, pain, and difficulty*". I hope this document and my understanding of the subject matter measures up to the standards to which you hold all of your students.

In regards to other students, I would like to thank my lab colleagues from MoRG, STRETCH lab, and beyond. From their individual skills and knowledge bases, I learned much of what I needed to complete this project. I am particularly grateful for the assistance of Roshelle Wijeratne and Anthony DiBerardino. Roshelle has consistently assisted my work and a second researcher to review all documents. She has been an essential asset to the project and crucial in the completion of this work. Also, Anthony has jumped into this research under my guidance with no hesitations or concerns.

Additionally, I would like to thank my committee and corresponding scientists, such as Bruce Orler and those within ICTAS. All have my thanks for their input and guidance within the complex subject field I chose to pursue.

Finally, this work could not have been completed without the constant support and help of my closest friends, family, and Shelly Rasnick. I wish you all the very best.

Table of Contents

List of Figures and Tables

Chapter 1: Introduction to Nonwoven Materials

1.1 Introduction

The market for nonwoven fabrics has experienced extreme growth in recent years and is expected to double in size from 2010 to 2020 [1]. This growth can be attributed to its numerous applications, ease of manufacturing, and customizable properties such as fabric stiffness, extensibility, and composition. The industries that use such fabrics span from the automotive and construction industries to the medical, consumer, and technology industries. Unlike a woven shirt, these spunbond nonwoven fabrics are produced by depositing extruded, spun filaments onto a collecting belt in a random manner, which are then connected by mechanical, chemical or heat bonds [2]. These bonding processes are faster than the manufacturing processes of traditional fabrics and allow additional freedom in product design. Consequently, the cost of production for a nonwoven fabric is much lower and more attractive than the woven alternative for many applications.

The ability to engineer a fabric opens up many possibilities for several industries. Nonwoven design ranges from single time use, such as disposable products like gauzes and wipes, to very durable products, such as agricultural coverings and upholstery. Demands of application when using traditional fabrics fuel the innovation within engineered nonwoven fabrics. Ultimately, these innovations originate from understanding and controlling the numerous production parameters to create products that are designed with properties comparable to or better than the woven alternative.

1.2 Production of Nonwovens

The production process of nonwovens varies depending on the application. Typically, fabrics are created for a specific job and, therefore, can achieve a good balance between the cost and product use-life. This balance is created by carefully varying each step listed in **Figure 1.1** shown below. It is important to note that each step has alternatives; however, **Figure 1.1** represents the leading processes to forming spunbond nonwovens to date [1].

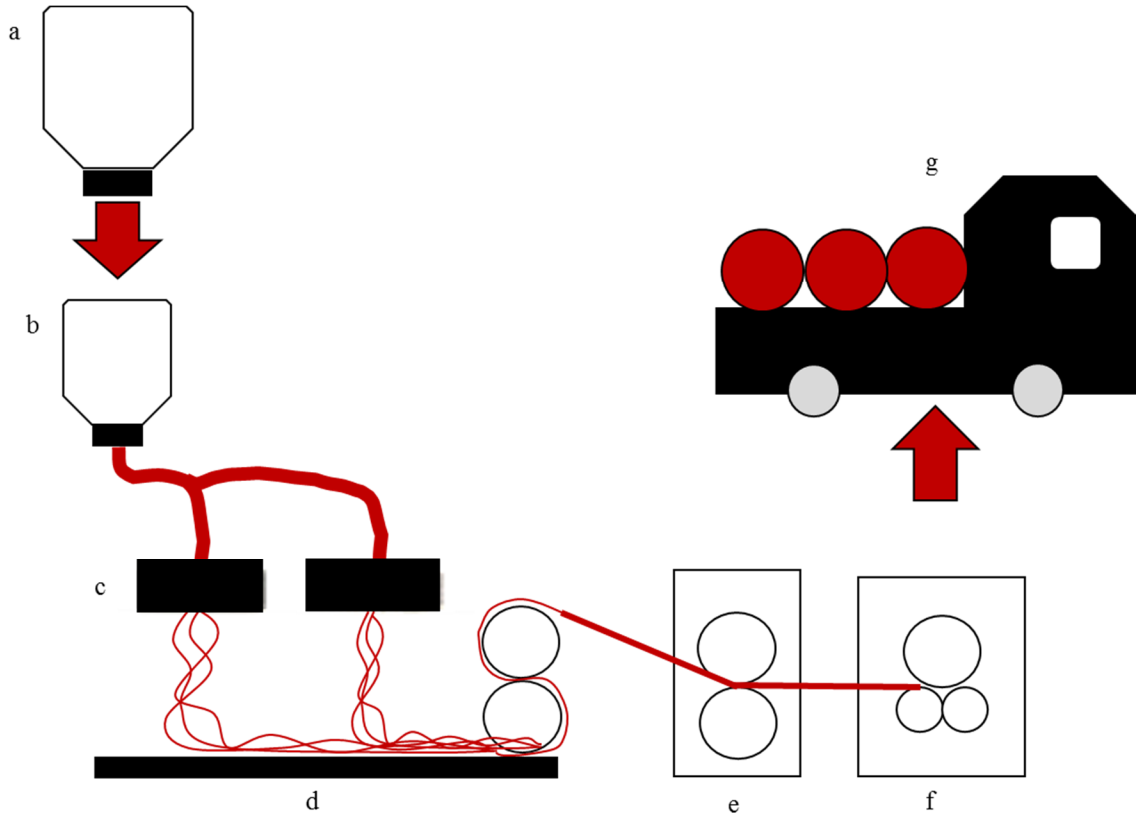

Figure 1.1: Processing of the nonwoven fabric.

a) Input of raw polymer(s) pellets. b) Extrusion of melted polymer. c) Spinning and fiber production. d) Creation of continuous web. e) Bonding process. f) Post processing. g) Customer delivery.

1.2.1 Fiber Formation

The processing of fiber formation is represented in **Figure 1.1 a, b,** and **c**. The first step involves choosing the input polymer or polymers. Different polymers have characteristic properties that can change the final fiber behaviors. For example, a polyethylene fiber provides a silk-like feel, which is desirable in certain Eastern cultures, versus polypropylene fiber that provides a warm cottony feel, which is desirable in certain Western cultures [3]. These polymers also exhibit different technical properties such as melting temperatures, melt viscosity, glass transition temperature and others that directly affect the cost of production. Consequently, polymers are chosen for several reasons pertaining to product design and can even be combined to create bi-component fibers.

Once a polymer or polymers are chosen, the input materials are melted and extruded (**Figure 1.1-b**) to the spinning and fiber production (**Figure 1.1-c**). Melting the polymer allows free movement of molecular chains, releasing any previous morphological order. These chains are then spun out at high rates to form fibers. The rate of spinning and cooling determine the degree of molecular orientation and crystallinity within fibers, another important characteristic for determining final fabric properties [4]. These continuously formed fibers allow various measures of control through varying the processing conditions, yet fiber formation only characterize the first half of the nonwoven production process.

Next the continuous fibers are laid onto a rapidly moving conveyor belt that acts as a bed for web formation (**Figure 1.1-d**). A web is the loosely entangled fibers that have not yet been imparted with mechanical integrity through bonding. The speed of the belt and number of fibers spunlaid determine the weight of the fabric and the degree of fiber direction anisotropy. Prior to web formation, the orientation of the fibers is random. Since

the belt is moving and the fibers are continuous, there is a preferential direction parallel to the belt direction, known as the machine direction (MD), and a non-preferential direction perpendicular to belt direction, known as the cross direction (CD). Consequently, the number of fibers and speed of the belt also determine the orientation distribution of fibers in the final product. At this point, the web is only held together by friction and inter-fiber entanglements. To create mechanical integrity, it is necessary to connect the fibers and transform the web into the fabric.

1.2.2 Bonding Process

The fibers are bonded together through multiple techniques – mechanical, chemical and thermal. Mechanical bonding involves either stapling fibers together or hydroentangling the web through water jetting. Chemical bonding uses an external adhesive to glue fibers together. Thermal bonding fuses fibers by heating components to temperatures near the melt so upon solidification fibers in close proximity are bonded [2]. Since the fibers themselves are auto-adhesive in thermal bonding, it is necessary that some constituent of the fiber be thermoplastic. The most common thermal bonding process, shown in **Figure 1.2**, is through applying local pressure under a heated calendar roll that thermoplastically bonds the web via conduction [5, 6]. This local pressure is applied from discrete nubs located on one or both of the calendar rolls. Thermal energy can also be transferred to the fibers through air (convection), radiation (infrared heating), and ultrasound (heat generation through vibrations) [5].

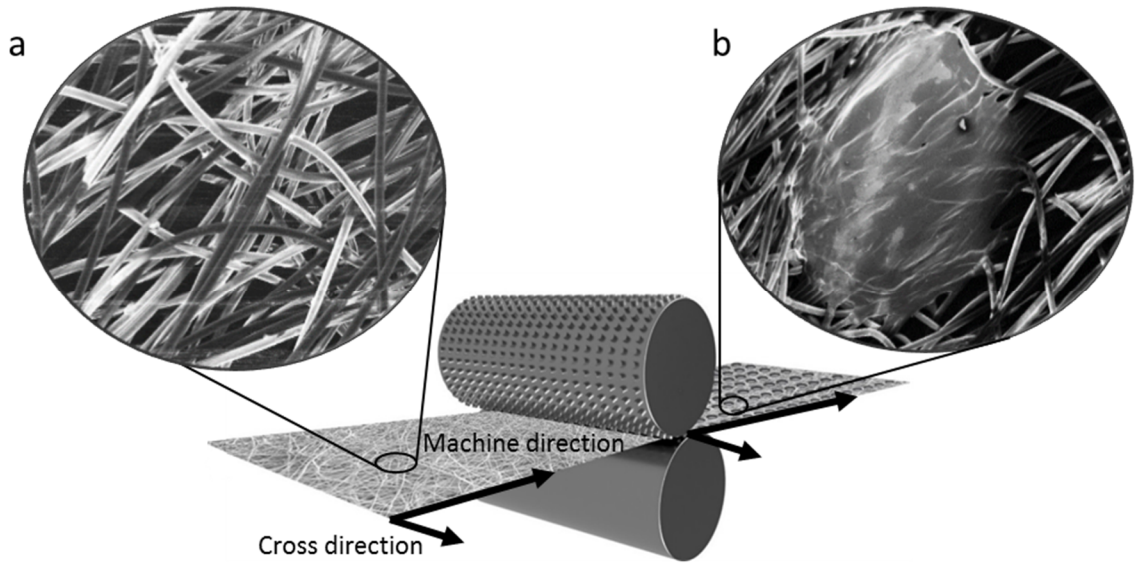

Figure 1.2: Schematic showing the thermomechanical bonding process.

First, a web of continuous random fibers (a) with no mechanical integrity is laid down. This web then travels through a heated calender roll with nips that transfer energy through heat and pressure to create a bond (b).

Once the web is transformed into a fabric through thermal bonding, the bonds are the essential structural feature imparting mechanical integrity to the nonwoven. These mechanical properties are of critical importance to product development and design for nonwoven applications [7].

After bonding, the fabric is post-processed and shipped to the customers. Post-processing involves cutting fabric to a uniform area and other various techniques to create desired final product such as purposely deforming the fabric, dyeing the fabric, or another technique. Therefore, post-processing and customer delivery are not expanded upon in this thesis. For the reader, it is important that post-processing typically involves some type of mechanical deformation of the fabric, intentional or not. Consequently, creating suitable final products involves a thorough understanding of mechanical and failure mechanisms of each processing step up to post-processing.

1.3 Motivation

There is a large push for companies to embrace sustainability throughout the life cycle of products due to previous mass production techniques of the 20th century that led to unforeseeable ecological consequences and expensive liabilities for the producers [8]. In terms of product design, this has created a shift towards material awareness and custom solutions for individual applications. To reduce cost and embrace sustainability movement, it is imperative for producers to prioritize material design and, therefore, research in material science and engineering.

Processing parameters such as bonding size, pattern, temperature, speed, and pressure allow industries to control the mechanical properties of nonwoven fabrics. However, manufacturers are currently unable to predict thermoplastic bond properties due to the limited or lack of knowledge regarding the bonding process. Without the ability to make a suitable prediction of processing parameters on the resulting quality of fabric, producers are forced to make new sheets in order to test parameters. This Edisonian approach requires significant raw material and additional hours of production time.

1.4 Goals and Objectives

The overarching goal of this research is split into 3 parts:

1. To gain an understanding of relevant data on the mechanical behavior of thermally bonded nonwoven fabrics
2. To systematically characterize constitutive properties of thermally bonded nonwovens

3. To understand failure modes with the objective of identifying metrics for bond quality “signatures”

More specifically, the focus of this study is to create a procedure to measure the mechanics and failure modes of a single thermomechanical bond site by taking into account the surrounding structure. The study details fast and simple analysis of the microstructure surrounding the bond site by measuring fiber density and fiber orientation then performing uniaxial tensile tests. The mechanical results are then coupled with morphological tests to gain full understanding of thermomechanical bonds. The insights have tremendous implications for the manufacturing process of nonwovens and will lead to more efficient use of the industry’s resources such as time, raw material used, and viable product fabricated.

Chapter 2: Literature Review of the Mechanics and Fracture of Thermomechanically Bonded Nonwoven

2.1 Fiber Properties

Understanding the characteristics of thermomechanically bonded nonwovens begin with understanding the basic constituent parts. Polymers, the molecular building blocks, are the starting point to understanding the countless variations in final products.

2.1.1 Influence of Polymer Morphology on Fiber Mechanics

Polymer nonwovens are typically produced by the extrusion spinning process, which requires thermoplastic polymer inputs. Man-made synthetic fibers have become the norm when creating these materials. While there are many types of synthetic thermoplastic polymers, this review will focus on the two of the most common types of raw polymer material - polyester and polyolefin [9].

Polyester fiber is a synthetic polymer composed of at least 85% by weight of an ester of a dihydric alcohol and an aromatic dicarboxylic acid [9]. Polyethylene terephthalate (PET) is an extremely common polyester, its structure is shown below in **Figure 2.1 a**. Polyolefin is a synthetic polymer composed of at least 85% weight of ethylene or propylene units [9]. The two unit structures are shown below in **Figure 2.1 b and c,** respectively.

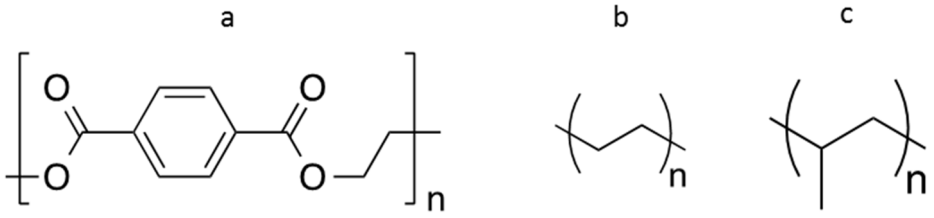

Figure 2.1: Chemical repeat structure of common nonwoven polymers.

a) Polyethylene terephthalate (PET), b) Polyethylene (PE) and c) Polypropylene (PP).

It is well established that the input polymer in making nonwoven fabrics has a significant effect on the resultant mechanical behavior. Hearle [10] examined a number of fibers in the 1960's and concluded that the polymer morphology gives rise to the structural mechanics within the fiber. Therefore, controlling the formation of fiber structure allows manufacturers to achieve desired technical properties within fibers. In the same decade, Samuels [11] examined the complex morphological deformation process that occurs during spinning and fabricating polypropylene fibers. Using a wide array of experimental techniques (small angle light scattering (SALS), wide angle x-ray diffraction (WAXD), micro x-ray diffraction (XRD), birefringence, interference microscopy, density and tensile measurements) after various processing variations, Samuels determined that the rate of drawing fibers alters how the polymer deforms and thus the resultant fiber mechanics. This relationship is true of both polypropylene and polyethylene, as shown by Spruiell and White [12] who studied changes in morphology compared to mechanical property changes in PE.

More recently, Osta et al. [13] examined the effect of fiber processing conditions on the mechanical properties of melt-spun polypropylene fibers. The study included subjecting different industrial polypropylene samples to manufacturing-relevant processing conditions and then examining their mechanical properties using uniaxial tension, creep, cyclic loading and strain rate sensitivity tests. The crystalline versus amorphous domains of the fibers were quantified through Raman spectroscopy using a method developed by Nielsen et al. [14]. The study concludes that fibers processed at higher uptake speeds strain harden more, have higher failure stress, and become more

brittle upon cyclic loading compared to those processed at a lower speed. An additional important deduction from this study is that fibers processed under the same conditions and made from nominally identical isotactic polypropylene (iPP) formulations demonstrated distinct differences when produced using different catalysts. Osta et al. note that the large range of variability in literature could thus have physical origins that are developed in structural features at sub-crystalline scale.

The intrinsic properties, such as melt temperature, viscosity, and glass transition temperature, greatly influence how the polymer is processed, how resulting fiber structure is formed, and the cost of production for manufacturers. Accordingly, manufacturers desire the lowest cost process for the final product. This is difficult to design when other factors, such as the sensation of the final feel of the fabric as noted in the introduction, affect which polymer types that are chosen. Fortunately, engineered nonwoven fabrics are not limited to a single component and current processing techniques allow for combining more than one polymer type.

2.1.2 Bicomponent Fiber Structure and Mechanics

Bicomponent fibers provide combined advantages of two polymer components. This type of composite fiber has been manufactured for over 50 years to increase desired fiber properties and have naturally occurring correspondences [9]. For example, wool is known for having a high molecular oriented, strong core and a low molecular oriented, hydrophobic sheath [15]. Forming a bicomponent fiber involves co-extruding two polymers from a single spinneret. The cross-sectional arrangement can be manipulated for the desired effect such as in **Figure 2.2** below illustrates the multiple cross-sectional

arrangements; it is a reconstructed figure taken from various sources that examined the various cross sections [15-17].

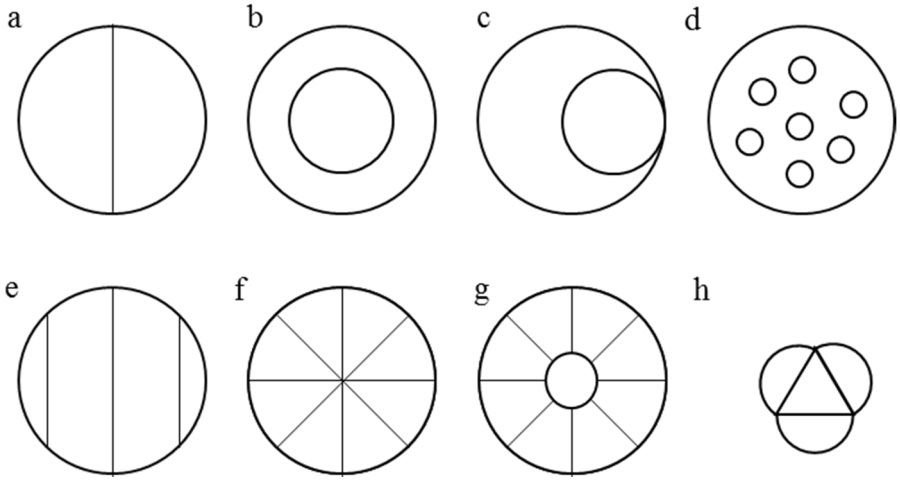

Figure 2.2: Types of bicomponent cross sections.

a) Side-by-side, b) concentric sheath-core (S/C), c) eccentric sheath-core (S/C), d) islands-in-the-sea, e) alternating layered, f) pies, g) citrus, h) and tipped tri-lobal.

The cross-section of bicomponent fibers influences many characteristics. Most commercially-produced and academically investigated bicomponent nonwovens have either concentric sheath/core (S/C) (**Figure 2.2 b**) or tipped tri-lobal (**Figure 2.2 h**) configurations.

By adding a second polymer component, the fiber morphology, structure, and mechanical properties become increasingly complicated. El-Shiekh et al. [18, 19] were pioneers in this topic, delving into theoretical predictions in the 1970s. The interactions between polymers were difficult to predict at this time due to relatively new techniques and, consequently, the theoretical agreement was inadequate to experimental results. Recent studies have come closer to understanding this relationship.

Dasdemir et al. [16] examined the polymer type and interface on the mechanical properties of sheath/core bicomponent fibers. The polymer compositions examined were

PET/PE, PA6 (polyamide 6)/PE, PA6/PP and PP/PE. They first examined the change in crystallinity, via wide-angle x-ray diffraction (WAXD), of two components with S/C composition ratios of 0/100, 50/50, 75/25, and 100/0. The authors postulated that the high melting temperature polymer, typically in the core, experienced improved consolidation stress and strain hardening that resulted in high percent crystallinity. Similarly, the low melting temperature polymer, typically the sheath, had suppressed crystallinity resulting from stress relaxation after the core solidifies. Using the Flory-Huggins interaction parameter and interfacial adhesion, the authors correlated deviations of mechanical properties to the compatibility of the two polymers. The polymers with negative interactions resulted in much lower mechanical properties compared to properties calculated from the rule-of-mixtures. Conversely, polymers with positive interactions resulted in higher mechanical properties. The interfaces are easily seen in **Figure 2.3**, which shows SEM photograph of the various sheath-core cross-section. They concluded that interaction of two polymers influences the resulting morphology and mechanical properties.

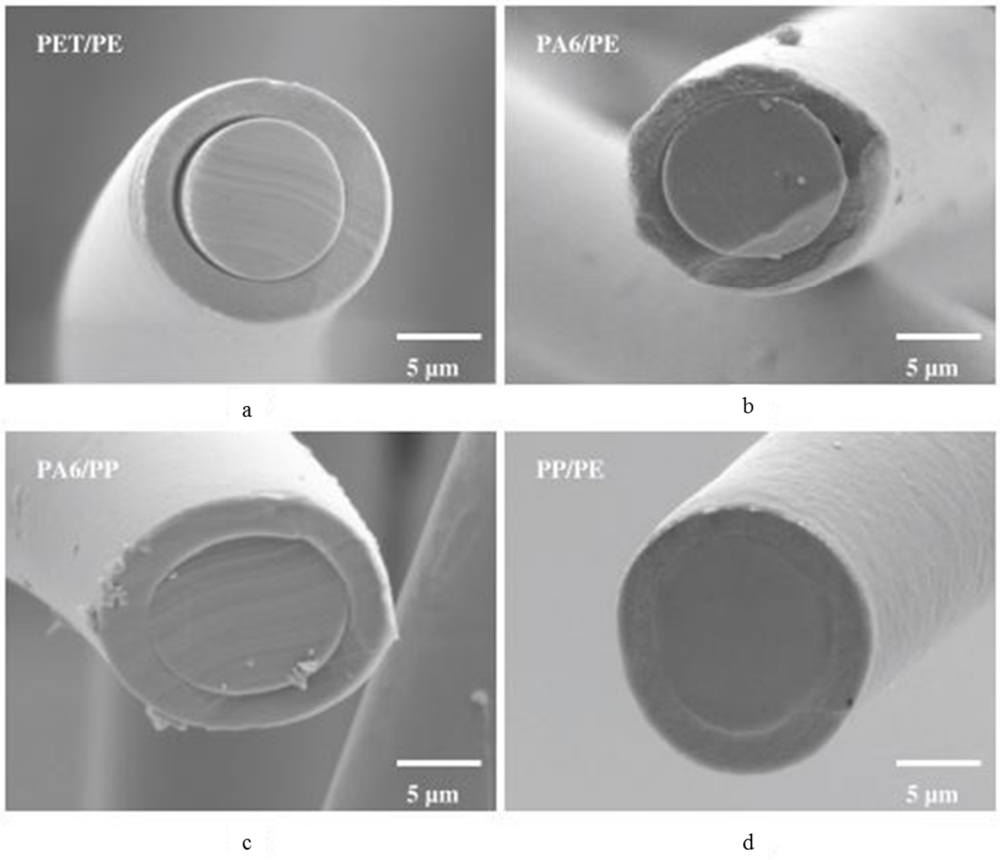

Figure 2.3: SEM pictures of bicomponent fiber cross-sections [16].

a) PET/PE, b) PA6/PE, c) PA6/P, and d) PP/PE.

Perret et al. [20] examined the polymer morphology within bicomponent fibers through WAXD and SAXS. The two polymers studied were PET and poly(phenylene sulfide) (PPS). Two-dimensional SAXS/WAXS patterns reflect the mutual influence of the components on their thermal profiles along the spinline. The authors concluded that the structure of the component that solidifies first is enhanced due to higher drawing while the less strain and delayed quenching gives rise to a more uniform crystal growth in the other component.

A key benefit of bicomponent fibers for producers is the ability to combine the characteristics of two polymers. A significant property is the melting temperature of a

polymer – a cost intensive property during production. Consequently, bicomponent fibers allow production of nonwoven fabric cheaper than single component fibers, for example by using a lower melting temperature component to cut down on the total energy. However, similar to understanding the relationship of morphology to mechanical properties, the thermomechanical bonding process is more complicated for bicomponent fibers than single component fibers, as discussed in **Section 2.2**.

2.2 Thermomechanical Bond Properties

After a web of fibers is produced, nonwoven fabrics may be generated through the thermomechanical bonding process. In order to better understand recent literature, it is necessary to examine the transformation from fibers to bond.

2.2.1 Formation of Thermomechanical Bond

The formation of a thermomechanical bond occurs in three steps [21]:

1. Compression and heating (a portion) of the web
2. Bonding (a portion) of the web, thus creating discrete bonds
3. Cooling of the bonded web

Polymer adhesion theory between multiple fibers best describes the thermomechanical bonding process. Polymer adhesion across an interface, in this case the separated individual fibers, occurs through complex diffusion and absorption phenomena [22, 23]. First, the two interfaces must wet and come into full contact with each other. At an elevated temperature, the polymer molecules can then mutually interdiffuse across the interface, thus becoming entangled within the opposite fiber. Upon cooling, the molecules solidify to create a mechanically stable bond. This molecular diffusion is dependent on the

temperature and time [24]. Consequently, it is necessary to reach a temperature that allows enough molecular movement within the time of the bonding process to create a mechanically stable bond. The time and temperature dependence of thermomechanical processing is shown below in **Figure 2.4**.

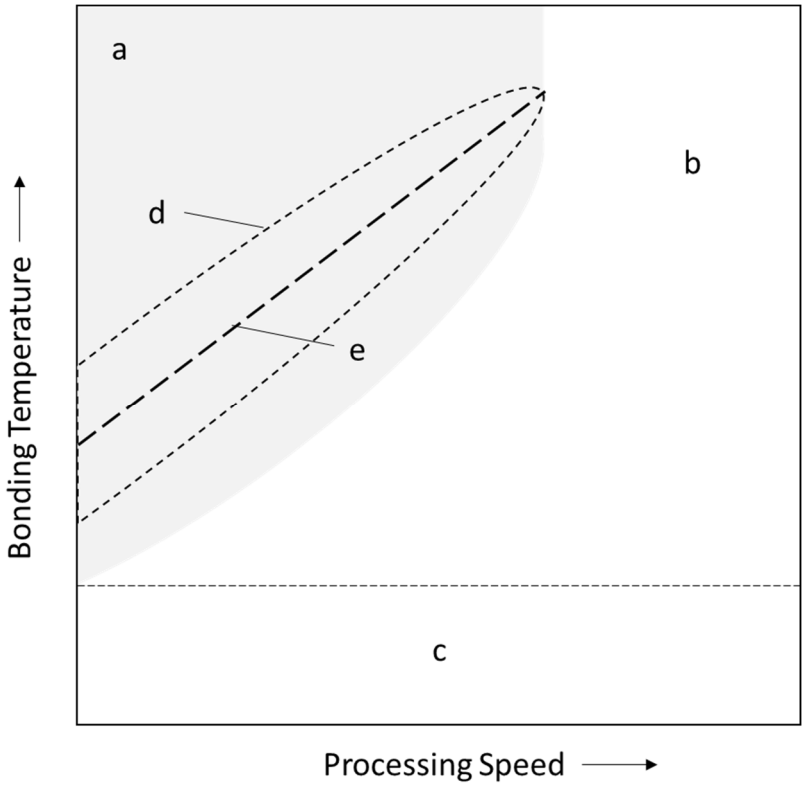

Figure 2.4: Processing window of thermoplastic bonds.

a) Mechanically stable bond formation. b) Processing speed is too fast to allow molecular movement. c) Temperature is too low for long range molecular movement. d) Acceptable bonding conditions (known as the processing window). e) Optimum bonding conditions.

If the bonding temperature is too low, or the processing speed is too fast, a mechanically stable bond will not form. On the other hand, if the temperature is too high, or the processing speed is too slow, the resultant bond will create a fabric with suboptimal mechanical properties.

Considerable effort has been spent on optimization within the bond formation to achieve known processing temperature windows for desired properties. At a single

processing speed, a low temperature will under-adhere the fibers, thus resulting in fibers only loosely connected. An optimum temperature will fully adhere the fibers as well as keep the desired mechanical properties of the processed fibers. A high temperature will result in fully adhered fibers, yet will lose the benefits from the specific morphological structure within the processed fibers. Dharmadhikary et al. [25] postulated that the maximum in fabric strength with increasing bonding temperature was the result of two competing effects, the increasing strength of bonds and decreasing fiber strength.

It is widely known that manufacturers can increase production speed to reduce cost; however, the temperature range of acceptable bond creation decreases. In other words, the difference between the minimum and maximum temperatures for acceptable bond creation decreases until the two merge into a single temperature; this is referred to as "closing of the processing window" [21]. **Section 2.2.2** and **Section 2.2.3** will delve into the properties, effects, and optimization of this "processing window".

2.2.2 Effect of Thermomechanical Bonding on Morphological and Mechanical Properties of Single Component Fibers

The thermomechanical bonding process significantly changes the fiber morphology imparted during spinning and, consequently, the mechanical properties. Over the past years, studies examined the influence of processing parameters on the entire nonwoven fabric properties. Indirectly, these studies give insight into the changes that occur on a microscopic scale as well.

Kim et al. [7, 26] showed the failure modes for nonwoven fabric made from polypropylene fibers at various bonding temperature and pressure. Large specimens (15 cm x 2.5 cm) were tested uniaxially in tension and imaged for failure analysis. Mechanical

properties of the specimen were greatly influenced by bond temperature and overall bond area, however, bond pressure showed little effect. The study concluded a change in the failure mechanism from fiber/fiber interfacial failure within the bonds at lower temperatures to bond/fiber interfacial failure at higher temperatures. This effect can be seen easily from optical images of sheet post rupture (**Figure 2.5**).

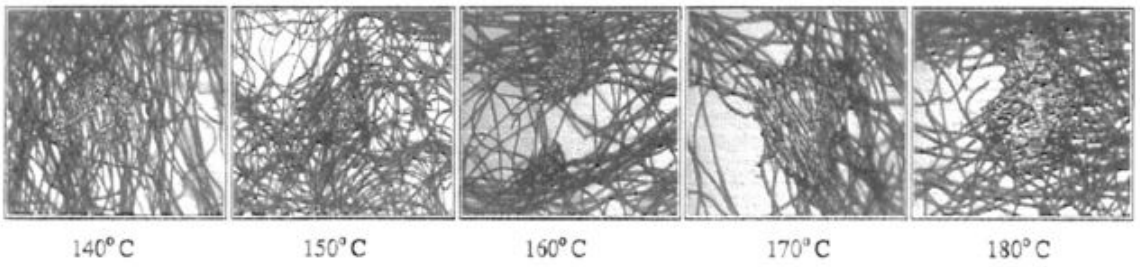

Figure 2.5: Rupture images of the bonded and surrounding domain as a function of bonding temperature [26].

The mechanical properties change significantly over the bonding temperature range, from 140°C to 180°C as shown in **Figure 2.6**. The principles of polymer adhesion theory can be seen from combining the visual failure from **Figure 2.5** with the force vs extension curves.

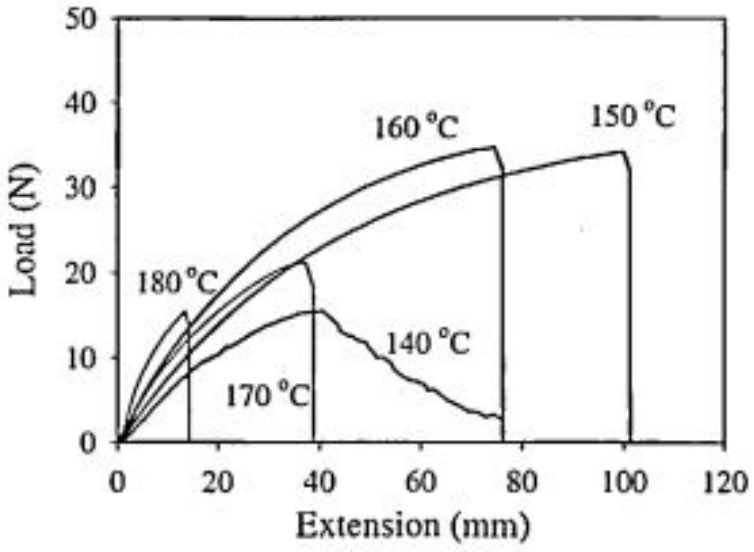

Figure 2.6: Typical tensile load-extension curves on bonding temperature series [26].

At the low temperature of 140˚C, the nonwoven fabric was under-bonded, which resulted in low maximum loads for the specimen. Medium temperature bonded specimen of 150˚C and 160˚C, reached the highest maximum loads and extensions. This represented the optimum thermomechanical processing window. Finally, at high temperatures of 170˚C and 180˚C, the nonwoven specimen reached low maximum loads, very low extension, and failed rapidly.

Brat et al. [27] conducted a similar experiment on the effect of bonding variables on the structure and properties of polypropylene nonwovens. The authors examined morphology through WAXD and additional mechanical properties such as tearing and bending tests on fabric specimen. Their results demonstrated that fiber morphology was unaffected through the bonding process and that bonded areas showed larger crystal sizes. However, the morphological data were not reported for variable processing conditions. Similar to previous studies, the fabric strength increased with increasing bonding temperature to a maximum then decreased with increasing bonding temperature. A bonding temperature of 150°C resulted in optimal properties. This trend of increasing properties to a maximum then dropping as bonding temperature increases has been observed extensively in the literature [5, 9, 28]. It is necessary to delve into the morphological changes that occur to better understand the optimum processing window for nonwovens.

Wang et al. [29, 30] developed a method of polarized laser Raman microspectroscopy and optical birefringence to measure the properties of polymer morphology, specifically the percent crystallinity and amorphous region. Once a correlation between Raman and birefringence was made, the percent of crystallinity of the polypropylene fiber, bond, and transition from fiber to bond could be measured. Wang et

al. concluded that the morphology of the bonds was considerably different from that of the original fibers, and the extent of the difference depends directly on bonding conditions. This conclusion followed logical thought regarding the changes resulted from bonding. However, the methodology for collecting Raman spectra did not account for changes in molecular orientation once into the bond, which has been shown to significantly impact the resulting spectra [31]. The instrument used was not a confocal laser and, therefore, penetrated through the full specimen. In this sense, the measurements started on single fiber morphology orientation than taken of multiple morphological orientations as the fiber entered the bond with multiple fibers. This change alone would result in changing spectra. The authors made no note of this transition and claimed all spectra differences were a result of changes in crystallinity. Consequently, the results that were drawn from Wang at el.'s Raman measurements should be interpreted considering these conditions and assumptions. This Raman technique has been the most widely quoted morphological measurement for variations in mechanical properties.

Chand et al. [32], additionally, investigated the role of fiber morphology on the thermal bonding process. Fibers were processed to create a large range of structures and then examined through differential scanning calorimetry (DSC), thermomechanical analysis (TMA), birefringence, and tensile testing of both fiber and fabric. The results indicated that the extent of change in fiber structure depends upon the structure of the original fiber and the process variables. In other words, different initial fiber morphologies bonded with different behavior. Fibers with high molecular orientation and crystallinity formed weak and brittle bonds due to a lack of polymer flow. Conversely, fibers with low tenacity and high elongations resulted in better bond creation. As a result, the fabrics with

constituent fibers of low tenacity and high elongations had higher fabric tensile properties, which the authors claim were due to the difference in failure mechanisms.

Faruhk et al. [33] examined how the change in morphology affected the mechanical properties of polypropylene fibers by creating a procedure for measuring the loss in the tenacity of fibers. **Figure 2.7** below shows the experimental setup. The test was conducted by clamping two bonds in an Instron mechanical testing machine with only one fiber spanning between each bond. The resulting uniaxial tensile test showed the mechanical properties of a fiber after thermomechanical bonding.

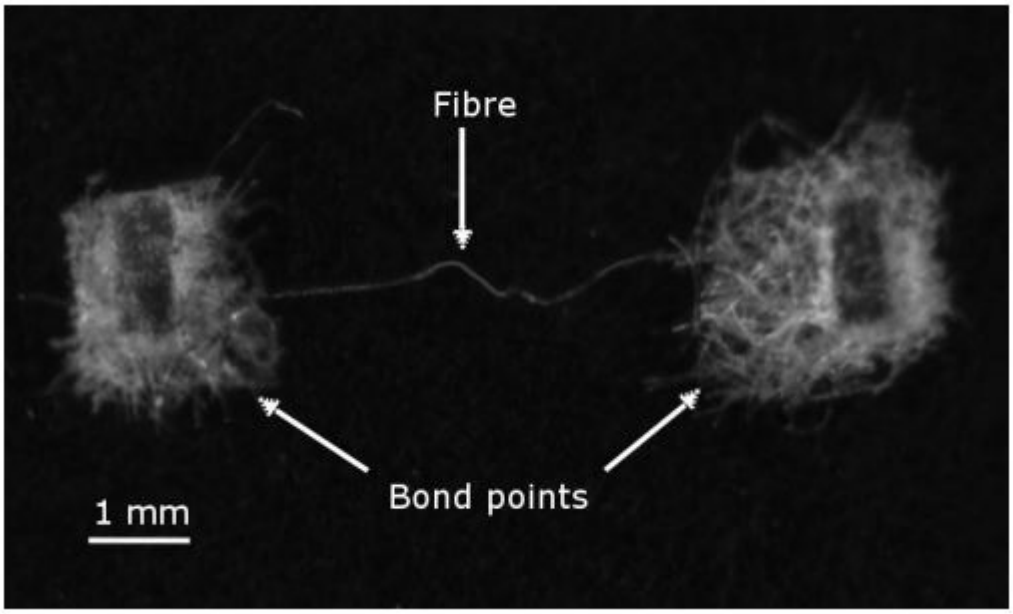

Figure 2.7: Experimental setup for measuring loss tenacity of fibers through thermomechanical bonding [33].

The findings conclude the breaking strength of polymeric fibers in the nonwoven at optimum processing conditions was less than that of virgin fibers, by approximately 50%, and claim this is a result of polymer morphology gradients near the bond edge. The authors note similar agreement to morphological tests conducted by Wang et al.[29]. Nevertheless, these tests lack clear insight to the bond itself.

The closest experiment to gain insight into the bond mechanical properties was developed in a doctoral thesis written by Chidambaram [34], although it was never published in a peer-reviewed journal. Two fibers were crossed at 45° then contacted with smooth rolls to form a bond. Control fibers were also produced without this bonding process. Mechanical tests were performed to calculate both bond fiber tenacity and bond strength, a diagram representation made by Chidambaram is shown in **Figure 2.8**.

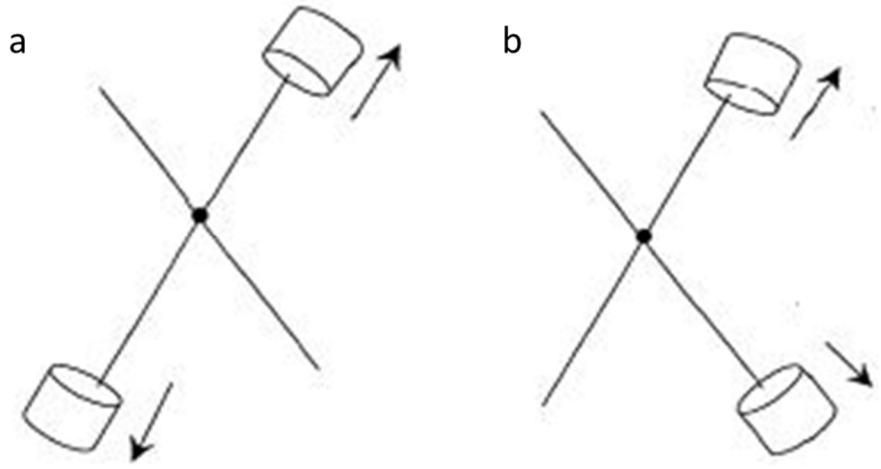

Figure 2.8: Mechanical testing of experimental thermomechanical bond [34].

a) Bonded fiber tenacity measurement and b) bond strength testing.

Chidambaram concluded that the bonding process causes the degradation of the component fiber strengths in the temperature range where significant bonding occurs. Mechanical damage due to compaction at bond points does not contribute significantly to fiber strength loss.

2.2.3 Effect of Thermomechanical Bonding on Mechanical and Morphological Properties of Bicomponent Fibers

The effect of thermomechanical bonding on mechanical and morphological properties of bicomponent fibers has not been studied extensively. Few experiments have

been performed on bicomponent fiber bonding and this is ultimately due to an inherent lack of knowledge within a single component system. Typically, bicomponent bonds are considered to be a composite consisting of a core fiber and the sheath matrix [35-37]. This can be an appropriate assumption when starting a model; however, the conjecture that the inherent core fiber properties remain the same while the sheath flows into a uniform matrix is far too simplistic. Especially considering the mechanical behavior of a single component bond is not completely understood. Further studies on bicomponent systems are necessary to develop an understanding of the effect of thermomechanical bonding on mechanical and morphological properties of bicomponent fibers.

2.3 Influence of Web Characteristics on Thermomechanical Bonding

The influence of web characteristics plays a significant role on how the bond sites are formed and, consequently, the resulting mechanical properties. The web can be produced at various densities, fiber orientations, and bond sizes and geometries.

2.3.2 Web Density

Basis weight is the most important parameter for defining the web of a nonwoven textile and represents the mass per area unit. Many properties including strength, thickness, porosity, tearing strength, etc. are influenced by changes in the basis weight of the fabric [21, 38, 39]. Due to manufacturers attempting to reduce cost and use more ecologically friendly processes, there is a large trend to decrease the basis weight of nonwovens [1]. This decrease in basis weight, and therefore the density of fabric, creates new obstacles that have not been discussed previously.

The material density directly affects the ability to optimally bond the nonwoven web. The primary heating process, as noted in the introduction, is through a conduction process. This means that the thickness of the material between nips correlates to the time needed to reach the optimal temperature. Consequently, samples' top and bottom layers may reach the optimum temperature while the middle never reaches an adequate temperature. Multiple studies have concluded this intuitive result of heating nonwoven fibers [7, 21, 26, 40]. Typically these studies correlate process speed to total time in nip and required time to heat nonwoven for a successful bond. The current trend for producing nonwovens is towards lower densities, which not only have less material but also can be processed faster for optimal bond creation [1].

As the amount of material decreases to lower basis weights, the amount of local non-uniformity increases. Low-density thermomechanical bonded nonwoven fabrics have a discontinuous and non-uniform microstructure, resulting in a complicated and unstable deformation mechanism. Hou et al. [41] studied this complex deformation process on 20 mm by 25 mm polypropylene fabric samples. The fabric had a density of 20 grams per square meter (gsm). Tensile tests and image analysis show that stress concentrates in the areas with a low local fiber density and that stress concentration transfers from one low-density area to another, generating shear stress in the specimen. These areas of non-uniformity can be as small as 2.0 mm by 2.0 mm, similar to the size scale of a common thermoplastic bond and its surrounding microstructure. An example of this nonuniformity is shown in **Figure 2.9** below.

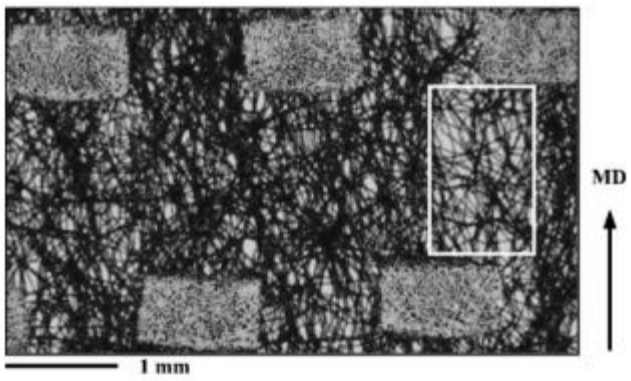

Figure 2.9: Non-uniform and discontinuous microstructure of nonwoven fabric [41].

The area with lower density is marked with a rectangle.

This study suggests that in order to characterize individual bonds the surrounding structure needs to be considered. With regards to the surrounding microstructure, many studies have probed the relationship of mechanical properties to the overall fiber orientation distribution. It is important to note, these studies are not limited to low-density nonwovens.

2.3.3 Fiber Orientation

Due to the processing technique of continuously laid fibrous material, nonwovens exhibit distinctive anisotropic behavior as examined by Kim et al. [26]. **Figure 2.10** below, reproduced by Michielsen et al. [21], visually shows the differences in mechanical properties depending on the direction of uniaxial tensile tests.

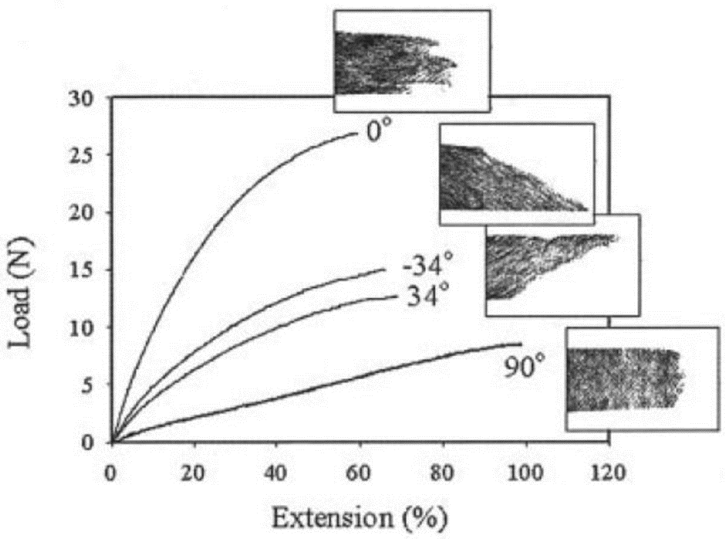

Figure 2.10: Angular mechanical properties of thermally bonded nonwovens [21].

The fabric fails by tearing across the fibers in the machine direction (0°) and in the cross direction (90°). For other test angles, the fabric fails by shearing across the preferred fiber direction (-34° and 34°).

Mechanical properties, such as failure mode of the nonwoven fabric, were dependent on the direction of loading compared to fiber orientation. This was because fibers were the principal load-transferring components. When the fibers were primarily aligned with the loading direction, MD, then the nonwoven could withstand the highest loads. On the other hand, the lowest loads the nonwoven could withstand were when the testing was perpendicular to the principal fiber direction, CD.

Fiber orientation distribution (FOD) function is a rapid, simple and useful tool for predicting the mechanical performance of nonwovens. There are multiple ways for determining FOD presented in the literature [7, 42-44]. These methods utilized an image of the nonwoven then derive the FOD. Typically, FOD is calculated once for the whole fabric and given as a histogram, such as in **Figure 2.11** below.

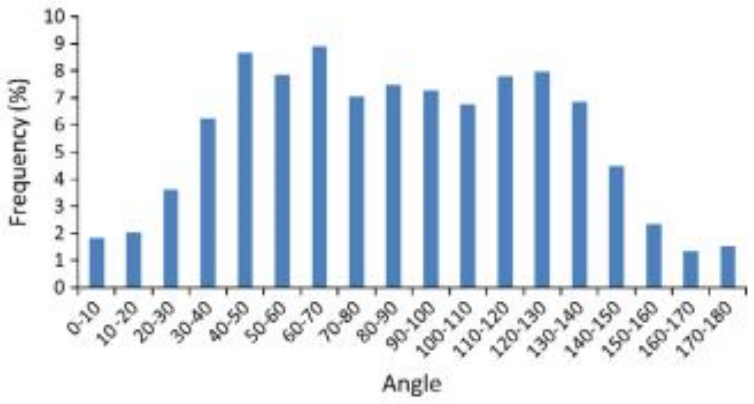

Figure 2.11: Typical fiber orientation distribution histogram [35].

PP/PE 35 gsm thermally bonded nonwoven (90° Corresponds to MD; 0° and 180° Corresponds to CD).

While this is fast and easy analysis, the results lack insight to the uniformity of the fabric do to the few number of measurements. The fiber orientation has the ability to vary across the nonwoven sample.

Rawal et al. [39, 45-47] have conducted considerable work regarding the theoretical and experimental determination of the fiber orientation, fiber volume fraction, number of fiber-to-fiber contacts, distance between the contacts, and porosity of thermally bonded nonwoven structures. The conclusions pointed to the significance of the nonwoven structure, especially when considering resulting mechanical properties. Furthermore, Amiot et al. [48] showed the correlations of structure parameters to multiple different measurements, namely tensile, air permeability, and compression measurements. Clearly not accounting for the variations in structure would result in suboptimal predictive models. In fact, this major drawback of the FOD becomes apparent when modeling nonwoven behavior.

2.4 Modeling Nonwoven Behavior

Modeling nonwoven behavior has been researched extensively. For this literature review, the models detailed will center on mechanics of bonds. The bond is treated as a rigid body or a composite calculated from bulk fabric properties [35, 49-51]. This assumption on the bonds leads to inaccurate results as shown by Kim et al. [40] since bonds have the ability to strain significantly. Subsequently, both rigid body and composite calculations result in insufficient predictions on the small scale (5 mm by 5 mm) mechanics of the fabric. This is because these bonds, typically less than 1.0 mm x 1.0 mm, have different failure mechanisms than the bulk material. If the fabric fails at these small scales, however, whole batches can be wasted during production and post-production processing. Similarly, calculations for bond properties lack the ability to predict mechanical changes from changing processing parameters. This is a direct result of a lack of understanding of the bond mechanics.

2.5 Gap in Literature Knowledge

Previous attempts to understand thermomechanically bonded nonwoven involve detailed analysis on entire fabric mechanics and the fibers but they provide little insight on the bond mechanics. There is no way to predict the resulting mechanical properties of a bond when changing processing parameters. The investigation of bond mechanics and the influence of each processing condition is challenging due to the numerous variables present within spunbond nonwoven fabrics. Consequently, the focus of this study is to create a

procedure to measure the mechanics and failure modes of a single bond by accounting for the surrounding structure thus reducing the intrinsic variation.

Chapter 3: Materials and Methods

3.1 Specimen Preparation

Commercially produced bi-component spunbond nonwoven fabric, made of polyethylene/polypropylene (PE/PP) at 20 g m-2, was obtained from a global roll-goods supplier. Four sheets of spunbond fabric, approximately 20 cm by 28 cm, were used: one was used only for basis weight analysis and three for basis weight, fiber orientation, and tensile testing.

Three sheets were laser cut into 120 bowtie specimens using an Epilog Laser Cutter (Epilog Mini 24 laser, Golden, CO, USA) set at rasta/vector, 90% speed, and 10% power. More precisely, the laser was only used to cut the clamping regions of the specimens and medical shears were used to isolate the bond in order to prevent damage of the bond due to heat from the laser. This provided consistent geometry of the specimens with notches that helped localize bond failure while allowing free movement of the surrounding fibers.

The bowties were cut with their longitudinal axes along three different directions in regards to the nonwoven: machine direction (MD), cross direction (CD), and between these two directions, diagonal direction (DD). Each sheet of fabric was used to isolate twenty bowtie specimen with the longitudinal axis along one direction. The specimens were selected based on the location of the bond after laser cutting. The bond was always located in the central region of the bowtie specimen to ensure load transfer through the bond during tensile testing. An example of three bowties are shown in **Figure 3.1** with the center bowtie containing an adequately placed bond for tensile testing.

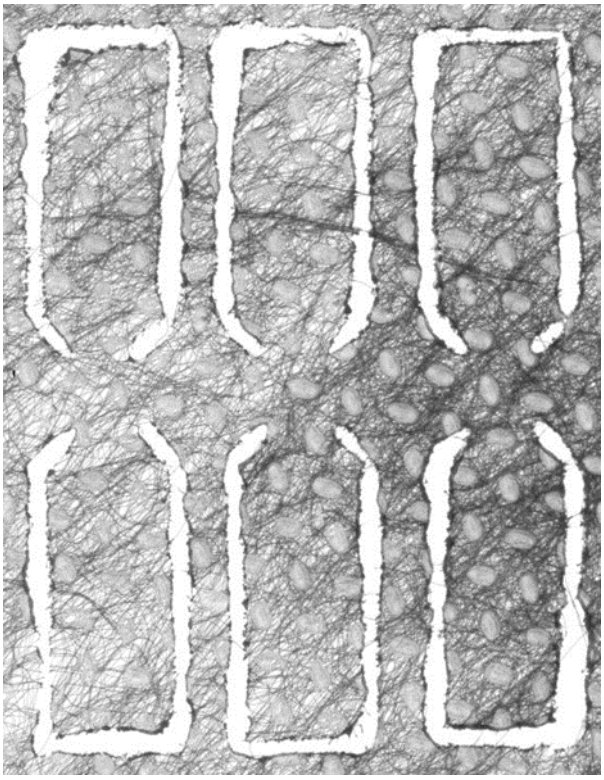

Figure 3.1: Digital scan of three bowtie specimen.

The center bowtie contains a bond in the proper location for further tensile testing.

3.2 Uniaxial Tensile Testing

Specimens (n=60) were loaded into a Nikon Eclipse LV100 microscope with an attached Linkam TST350 tensile stage (20 N load cell with a 0.01 N resolution) (**Figure 3.2**).

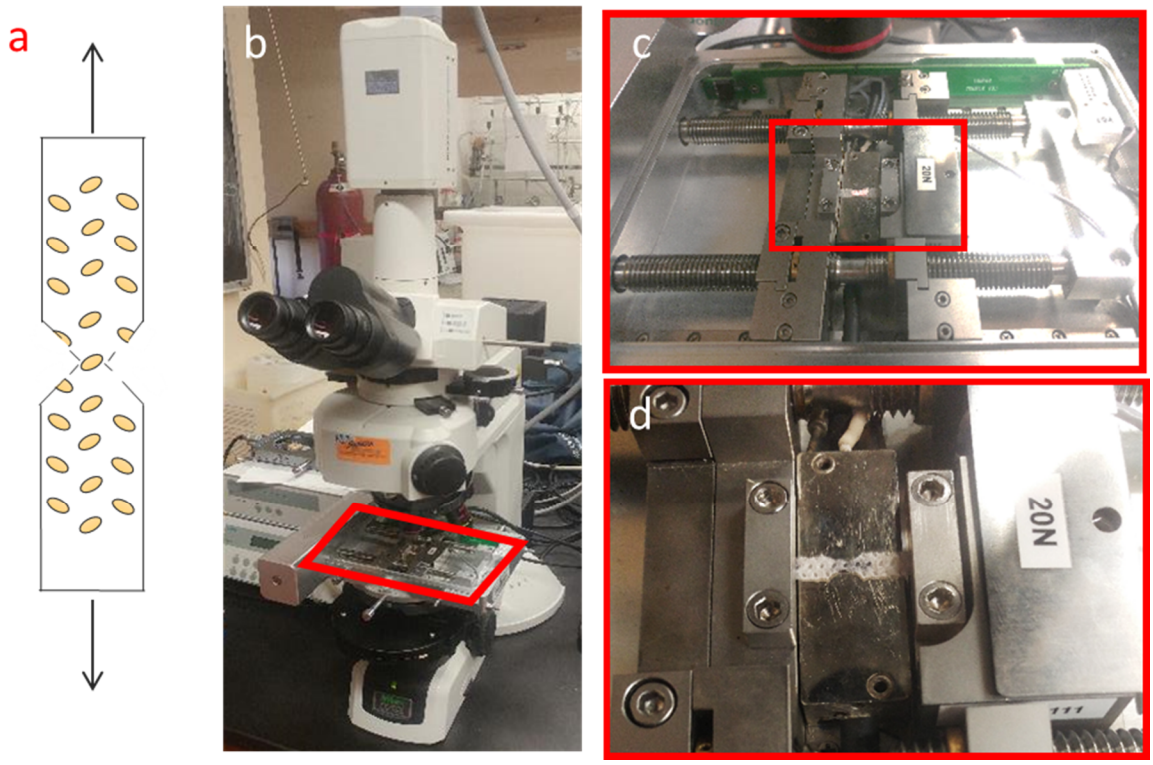

Figure 3.2: Schematic showing testing set up.

(a) Bowtie specimen and loading direction. (b) Microscope, camera, and tensile stage. (c) Tensile stage. (d) Clamped specimen.

During mechanical testing, the microscope was set to 40X view with automatic capture taking an image every 2 seconds. The specimen was lit from below with cross polarization and quarter phase shift. This light scheme was chosen because of the consistent ability to visualize the fibers and bond throughout testing. Each specimen was tested at constant extension rate of 40 μm/s at room temperature. The specimen was preloaded to 0.01 N prior to data acquisition. Force and displacement data were collected together with corresponding specimen images.

3.3 Analysis

3.3.1 Basis weight and Orientation

All the four spunbond nonwoven sheets used in this study were scanned using an optical transmission scanner at a scanning resolution of at least 2400 dpi after laser cutting three of the sheets. Both basis weight and fiber orientation analyses were measured using ImageJ software (National Institute of Health; Bethesda, Maryland, United States). More specifically, a square area approximately 1.5 mm by 1.5 mm inside the laser cut area containing a bond at its center, was selected as a region of interest for basis weight and fiber orientation measurements for all the specimens that were mechanically tested.

Similarly, 10,000 squares, each having a 1.5 mm by 1.5 mm area, were used as regions of interest to measure the basis weight from the non lasercut sheet of fabric. Basis weight was calculated by using the Beer-Lambert law, according to which light transmitted through the nonwoven is given by:

$$I = I_0 e^{-\mu\rho L} \quad (1),$$

where I_0 is incident light, μ is the mass-absorption coefficient, L is the thickness of the nonwoven, and ρ is the density of the nonwoven. Since ρL is mass per unit area, or basis weight (B), Equation (1) is modified as:

$$I = I_0 e^{-\mu B}. \quad (2)$$

Upon re-arrangement, Equation (2) becomes,

$$B = \frac{1}{\mu} l\, n \left(\frac{I_0}{I}\right). \quad (3)$$

Equation (3) provides basis weight of the nonwoven at any location based on a given I_0, I, and μ. I_0 and I were measured from the transmission scanner from region with and without the nonwoven, respectively. However, the mass absorption coefficient μ is constant material property that was not readily measurable or available. Therefore, basis weights of different regions within the same nonwoven was compared. This was done by computing

the values of B μ which vary from 0.0 to 1.0, where 0.0 indicated no material present in the region of interest and 1.0 indicates the material occupied the entire region of interest.

The orientation distribution of fibers around the bonds in mechanical testing was computed via direction of the intensity gradient [52]. The analysis was done using the OrientationJ plugin (École Polytechnique Federale De Lausanna; Lausanna, Switzerland). The scanned image was first aligned to the principal machine direction (MD) corresponding to 0° in the software, and then filtered to smooth the image in order to remove any fine scale noise, such as any undesirable fine scale topography on the bond surface within the width of a fiber diameter. This was accomplished by running a Gaussian Blur procedure at the fiber diameter of 17 μm. Fiber orientation distribution was evaluated by calling the OrientationJ plugin and calculating a structure tensor at 1.5 times the fiber diameter.

The orientation distribution allowed for an orientation parameter, O_p, to be calculated in comparison to the direction of the tensile tests. Defining the orientation distribution as $f(\theta)$ resulted in the ability to use Equation (4) from Cox's [53] analysis strength of fibrous materials:

$$O_p = \frac{\int_{-\pi/2}^{\pi/2} f(\theta) Cos^4(\theta) d\theta}{\int_{-\pi/2}^{\pi/2} f(\theta) d\theta} . \quad (4)$$

It is important to note that 0˚ was defined as the primary loading direction in the uniaxial tensile tests. This results in a parameter between 0.0 and 1.0, where 1.0 indicated that the fiber was aligned perfectly along the loading direction.

3.3.2 Uniaxial Tensile Analysis

The force-displacement data (and corresponding images) of the specimens were collected. For each specimen, the maximum force achieved and the stiffness were

calculated. The stiffness was calculated by considering the force-displacement data collected from the specimens stretched up to 0.3 mm displacement. This region of the force-displacement curve was determined to be the initial linear elastic region for all specimens. The average and standard deviation were also computed for the whole curve in each testing direction (MD, CD, and DD).

The image sets were analyzed and three modes of failure were examined. These were bond yield, fiber breakage, and bond cohesive fracture. If a visual change in bond geometry was observed, than this was interpreted as a yielding of a bond. Fiber breakage was easily detected when a fiber broke and left the image field of view. Lastly, bond cohesive fracture denoted failure within a bond (e.g. tearing of the bond into two or more parts).

One-way analysis of variance was conducted to compare the mean of stiffness and maximum load for the MD, CD, and DD. The student's t-test was used and the threshold chosen for statistical significance was 0.05 for comparing the percentage of occurrence for bond yield, fiber breakage, and bond cohesive fracture. Data were analyzed using the JMP statistical software (JMP, Version 10, SAS Institute Inc.).

Chapter 4: Results and Discussion

The specimens oriented along the MD experienced failure within the bond under tensile loading. **Figure 4.1** shows a representative image set for the specimens along the MD. More precisely, **Figure 4.1-a** presents the start of the tensile test (gage displacement was 0.0 mm) once the specimen was pre-loaded to 0.01 N. In each of following images (**Figure 4.1-a** to **4.1-i**) the specimen length increased by 0.8 mm increments over a time interval of 20 seconds. As the load increased, the bond re-oriented itself along the loading direction and deformed significantly in such direction (**Figure 4.1-c**). In **Figure 4.1-d** one can observe that the bond was sheared along the loading direction and separated in two parts. This denotes cohesion failure within the bond. After such failure (**Figure 4.1-i**), the bond was successfully transmitting load despite having fractured into two separate parts and there were still many fibers holding the load. This type of bond deformation and failure was commonly observed in the MD. Most importantly, the bond allowed distribution of load to multiple fibers. At a 6.4 mm displacement (**Figure 4.1-i**), fiber failure was not usually detected. This was strictly different from what was observed for specimens loaded along the CD.

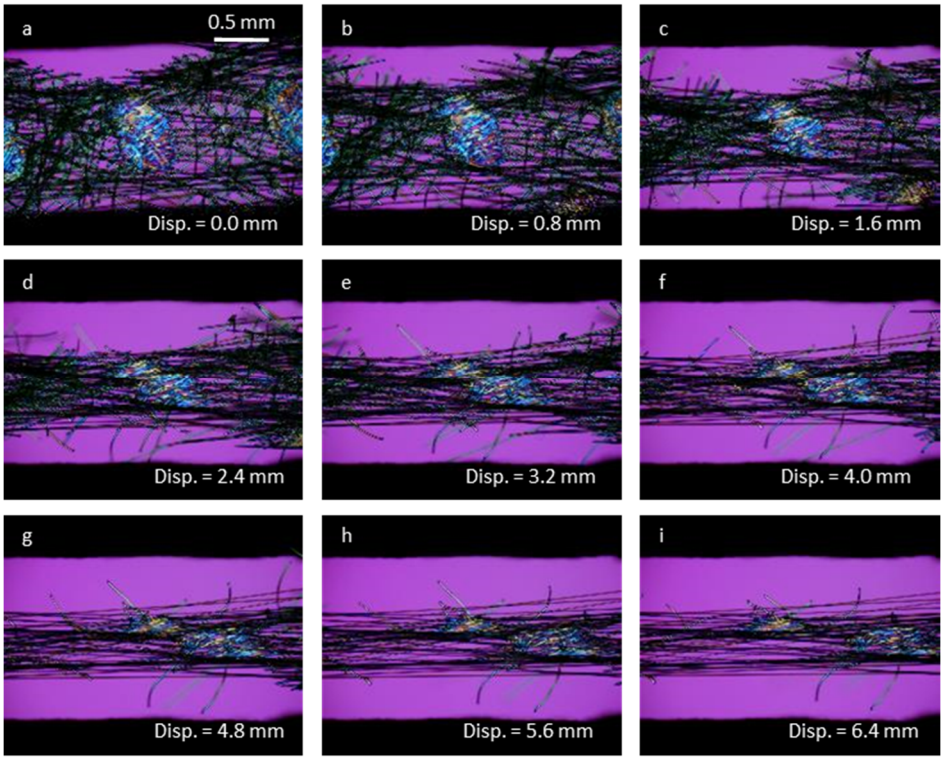

Figure 4.1: Micrographs of a representative bowtie specimen loaded along the MD at different displacement values (from 0.0 to 6.4 mm) illustrating bond deformation and cohesive failure.

The specimens subjected to tensile tests along the CD displayed individual fiber failure with no bond deformation. **Figure 4.2** presents a representative image set for a specimen loaded along the CD. The images were collected at the same displacement values used above from 0.0 mm to 6.4 mm. Although the load increased, the bond did not deform or reorient significantly (**Figure 4.2-c**), in contrast to what occurred for the specimen loaded in the MD (**Figure 4.1-c**). In **Figure 4.2-c**, two fibers transferring load within the bond can be observed. Then, in **Figure 4.2-d**, only one fiber transferring load can be detected. This indicates individual fiber failure. After a displacement of 2.4 mm, the number of fibers attached to one site of the bond decreased and the fibers on such site deformed more. The bond no longer had a comparable number of fibers attached to both of its opposite sites along the CD. When the displacement was 6.4 mm (**Figure 4.2-i**), there

were fewer than 10 fibers holding load on one site of the bond and the bond did not display any deformation. It was uncommon for the bond to deform or experience failure for the specimens loaded along the CD. Individual fiber failure was the primary mode of failure for these specimens, even at gage displacements as low as 2.4 mm (**Figure 4.2-d**).

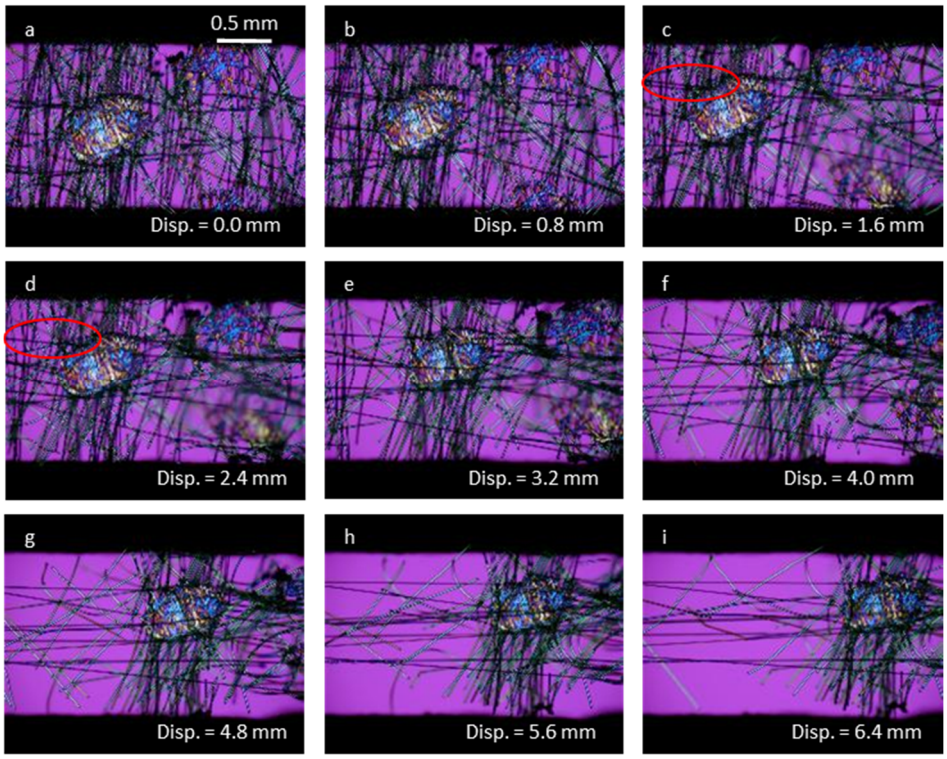

Figure 4.2 Micrographs of a representative bowtie specimen loaded along the CD illustrating fiber failure and no bond deformation.

The red circles in (c) denote the presence of two fibers and in (d) the failure of one of these two fibers.

The specimens that were tensile tested along DD primarily displayed individual fiber failure with minimal bond reorientation and deformation. **Figure 4.3** shows an image set for a representative specimen loaded along the DD. Again, images were collected as described above. The bond did not deform or reorient significantly by **Figure 4.3-c**, similarly to the bonds within the specimens loaded along the CD. As the displacement increased (**Figure 4.3-f**), the visual size of the bond decreased as the bond curvature

changed. There was no significant in-plane bond deformation or failure. Similar to what occurred for the specimens loaded along the CD (**Figure 4.2**), the bond did not have an equal number of fibers on both its sites. Additionally, the number of fibers attached to the bond decreased (**Figures 4.3-f** to **4.3-i**). This indicated that individual fiber failure occurred starting at 5.0 mm displacement.

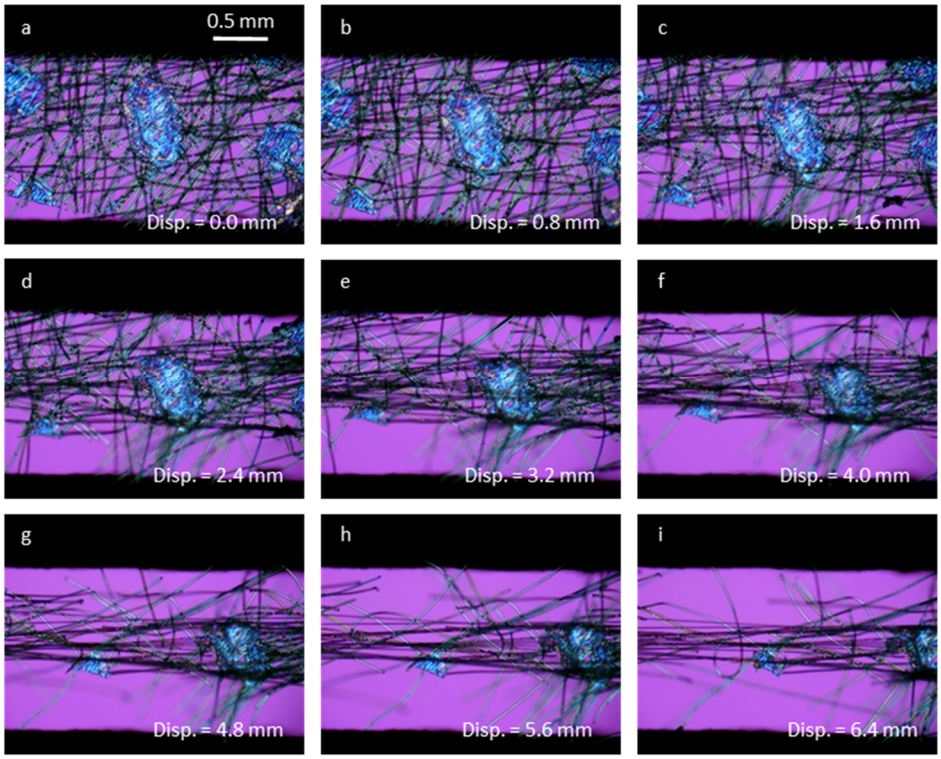

Figure 4.3: Micrographs of a representative bowtie specimen loaded along the DD illustrating fiber failure and minimal bond deformation.

A qualitative comparison of the results indicated that the bond's mechanical response was dependent on the loading direction. All the specimens tested exhibited individual fiber failure. However, bond deformation and failure was not common across all the specimens. Statistical analysis through t-tests revealed the occurrence of bond deformation was statistically significant within the specimens loaded along the MD compared to specimens along the CD, and DD with p-values less than 0.0001 and 0.0003,

respectively. This means that the occurrence of bond deformation was dependent on the loading direction. The likelihood of bond deformation was highest for specimens in MD, occurring 95% of the time, and lowest for specimens in CD, occurring 35% of the time. This denotes the importance of fibers to serve as load transfer for the bond. Indeed the individual bonds were clamped using the fibers connected to it. Similarly, the occurrence of bond failure decreased from MD to CD. However, the statistical analysis showed there was no significant difference in the occurrence of bond failure among the specimens tested along the MD, CD, and DD. This was likely due to the intrinsic variability in the structure of the tested bonds. Moreover, the non-uniformity within low-density spunbond fabric is very high and affects the ability to classify the bond deformation and failure and interpret its mechanical properties.

The wide range of bond characteristics resulted in specimens that exhibited a wide variation of mechanical behavior. **Figure 4.4** displays a specimen tested along the MD that was extremely different than the previously shown representative specimen (**Figure 4.1** to **4.3**). One can observe that, due to the low density of fibers, there were voids created in the bond during the production process. There was a significant bond deformation at 2.4 mm displacement (**Figure 4.4-d**) and the bond disintegrated at 5.6 mm displacement (**Figure 4.4-h**). This was different from what happened for the representative specimen tested along the MD which exhibited significant bond deformation and ability to transfer load after a displacement of 6.5 mm (**Figure 4.1**). This high degree of variation was evident within the quantitative mechanical results.

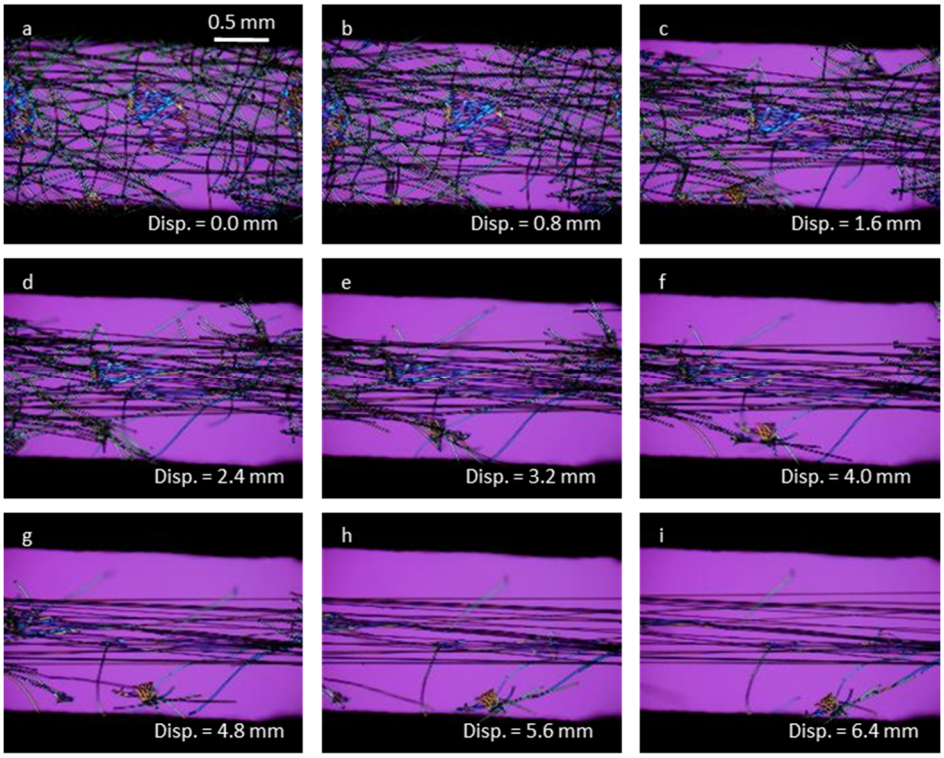

Figure 4.4: Micrographs of a bowtie specimen loaded along the MD illustrating how the variability in the specimen structure (e.g. lack of fibers within the bond) leads to bond deformation and failure mechanisms that were different from those observed in Figure 4.1.

The ability of a bond to support load was greatly influenced by the loading direction. However, even within specimens tested along the same direction, there was a large degree of variation in the bond mechanical response. **Figure 4.5** displays the average force versus displacement curves with the standard errors for specimens oriented along the three different tested directions. The load for the specimens tested along the CD reached just over 0.1 N while it attained 0.2 N for the specimens tested along the DD and extended over 0.4 N for the specimens tested along the MD. This increase in load trend can be seen within the initial linear region of the load-displacement curve as well. Correspondingly, t-tests confirmed that the maximum force and stiffness were significantly different among the specimens tested along the MD, CD, and DD. The importance of loading direction on

the mechanical data was consistent with previously reported studies. Nevertheless, the average curve for CD specimens was within one standard deviation to the average curve for DD specimen from 5 mm to past 10 mm displacements. This kind of variation makes comparing processing parameters extremely difficult. The first portion of the load-displacement curve, shown in **Figure 4.6**, indicated that the variability even influenced the linear regions of the curves. The difference in bonds, such as those shown in **Figure 4.1** and to **Figure 4.4**, led to standard deviation within specimens tested along the same direction to reach over 50% at specific displacements. This shows the extreme intrinsic variation within low density nonwoven fabrics, such as the one studied. When analyzing new processing methods, understanding the result of this variation is imperative to ensure differences are due to variation in the process and not due to the intrinsic variation.

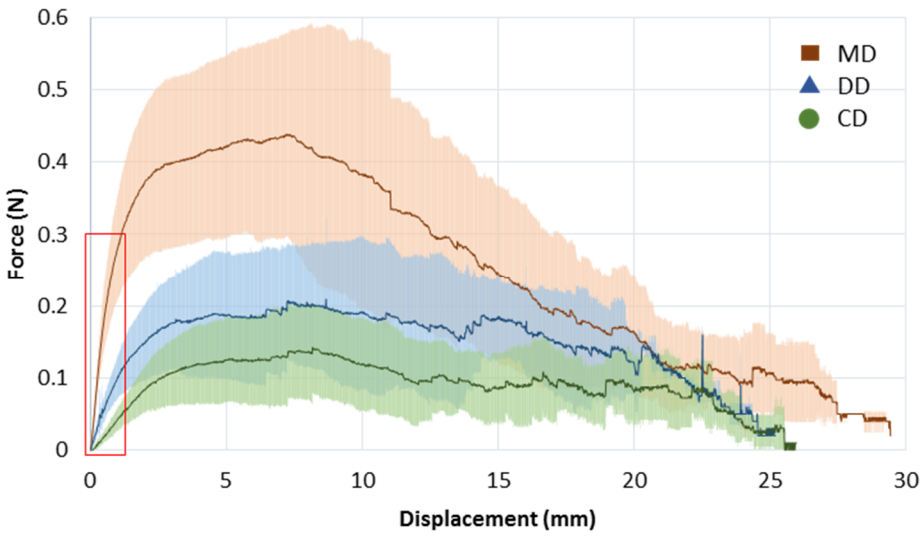

Figure 4.5: Average force versus displacement curves with standard errors collected from specimens tested along the MC (n=20), DD (n=20), and CD (n=20).

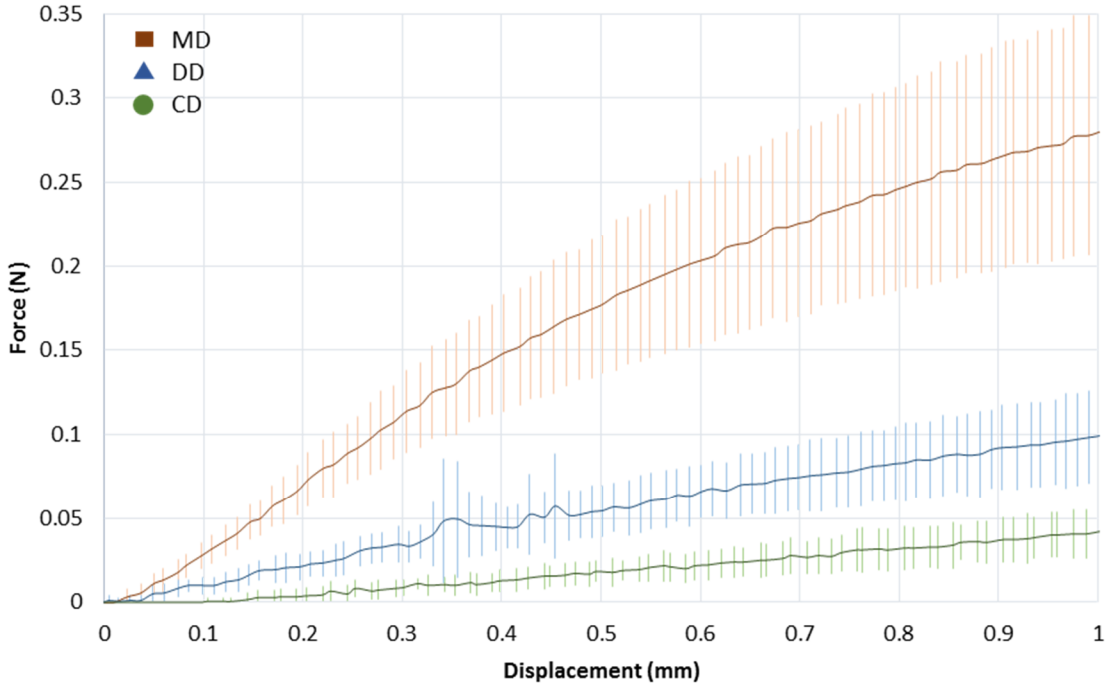

Figure 4.6 Average force versus displacement curves with standard errors collected from specimens tested along the MC (n=20), DD (n=20), and CD (n=20). The data reported here are those reported in Figure 8 up to 1 mm displacement.

Fiber orientation of spunbond nonwoven fabrics has been used widely to understand the differences in mechanical properties. However, such fiber orientations were typically calculated as a bulk property without accounting for variation of the size of regions selected for the measurements [28, 10]. However, the variations of fiber orientations were significant when considering single bonds. **Figure 4.7** shows four groups of fiber orientation distributions. **Figure 4.7-a** illustrates how the fiber orientation changes depending on the area considered for measurement. The fiber orientation for a large area differed significantly from the fiber orientation surrounding a single bond. **Figure 4.7-b** displays the fiber orientation distributions for all the specimens (n=20) along the MD. The distributions were always centered on 0˚. However, the spread of the distribution changed

significantly (**Figure 4.7-b**). The front specimen distribution reached a maximum frequency below 20% while a specimen distribution in the back touched 40% at its maximum. This variation was within each testing direction of DD (**Figure 4.7-c**) and CD (**Figure 4.7-c**). Correspondingly, the density of fibers also varied significantly throughout the specimen such as **Figure 4.4** demonstrated with many voids in the bond due to lack of fibers

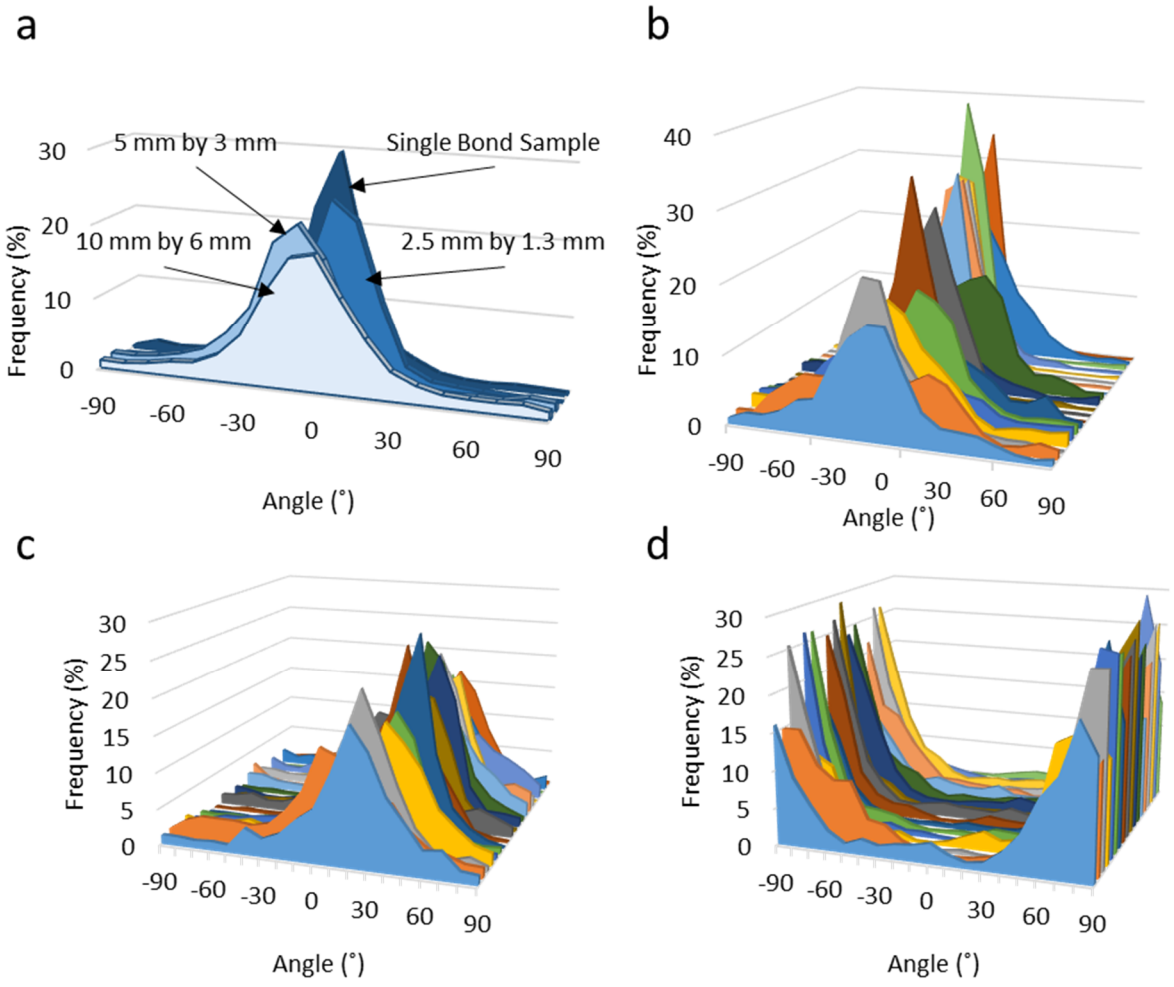

Figure 4.7: (a) Four fiber orientation distributions for four different sizes of specimen area scanned (10 mm by 6 mm, 5 mm by 3 mm, 2.5 mm by 1.3 mm, and single bond). (b) Fiber orientation distribution for MD specimens (n=20), (c) Fiber orientation distribution for DD specimens (n=20), and (d) Fiber orientation distribution for CD specimens (n=20).

A degree of variation was calculated for the density of fibers as well. Basis weight was used to measure the relative density of fibers surrounding a bond. **Figure 4.8** shows two frequency histograms binned at every 0.01 from 0.00 to 1.00. The orange histogram represents 10,000 basis weight measurements from one sheet and the blue shows 60 basis weight measurements, each from one specimen used within this study. The basis weight measurements from one representative sheet indicated that the specimens chosen for mechanical testing were representative of the whole nonwoven fabric. The density variation was extreme, ranging from 0.16 all the way to 0.76. The orientation distributions alone could not account for variation in the amount of fibers. Nevertheless, it was important

to understand the range of possibilities within each direction tested.

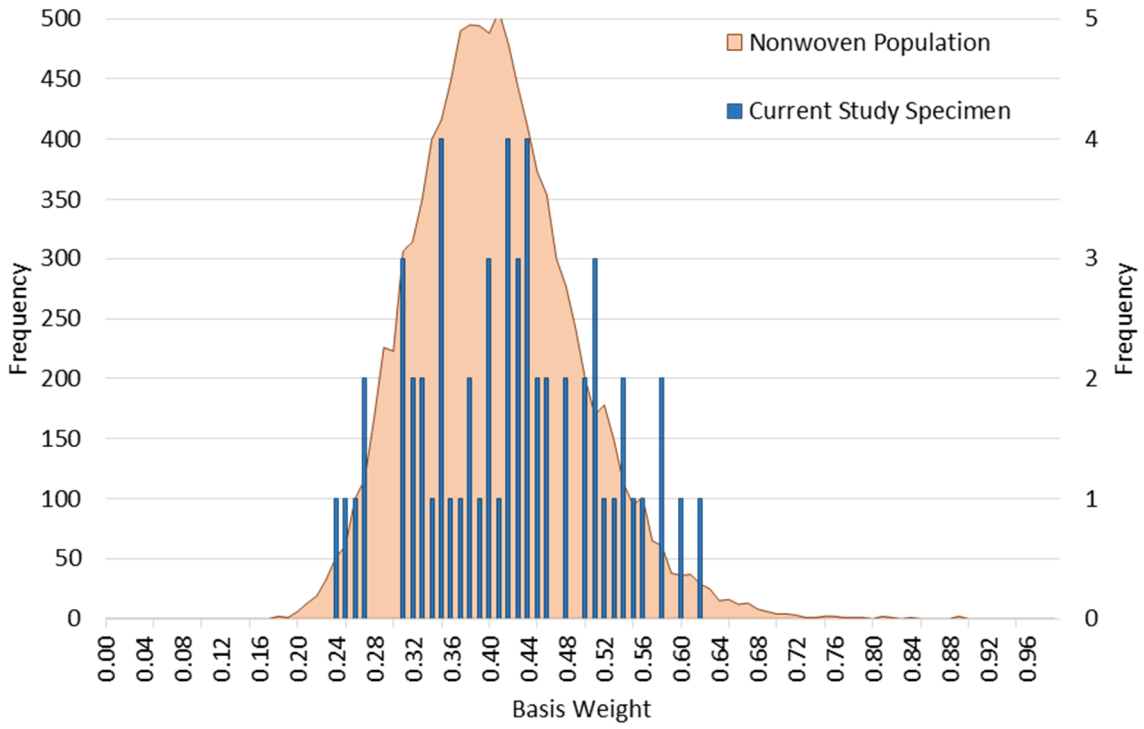

Figure 4.8: Basis weight distributions from spunbond nonwoven fabric (orange) and from all tested specimens (blue).

Table 4.1 shows the averages and standard deviations of the orientation and basis weight parameters for all specimens in each of the three directions. The orientation parameter was the highest for specimens tested along the MD and it was lower for those tested along the DD and CD, respectively. This was expected because the fibers were mainly aligned along the MD during the production process. It was important to note that the average basis weights in all directions were similar. Statistical analysis through t-tests proved that the basis weights for the testing directions were not significantly different. The standard deviations for these parameters were quite large indicating the large variation of the specimens. Nevertheless, it was important to note that, within one direction, one

standard deviation from the mean can vary the basis weight from approximately 0.3 to 0.5. This difference played a significant impact on the resulting mechanical properties.

Direction	Orientation Parameter (Average)	Basis weight Parameter (Average)
MD	0.772 ± 0.102	0.405 ± 0.097
DD	0.190 ± 0.048	0.416 ± 0.096
CD	0.078 ± 0.029	0.461 ± 0.083

Table 4.1: Parameter averages and standard deviations for all specimens tested.

The local fiber orientation in combination with the number of fibers surrounding a bond influenced the resulting mechanical properties. **Figure 4.9** shows the correlation of orientation parameter multiplied with basis weight parameter to stiffness. At low orientation and basis weight parameter, the stiffness of the system was low. As the orientation and basis weight increased, so did the specimen's stiffness. Within a single testing direction MD, the stiffness increased from 0.25 N mm-1 to 0.50 N mm-1 and correlated to the change in fiber orientation and fiber basis weight. The ability to transfer the load through the bond was attributed to the number of fibers (basis weight) and the direction of those fibers (orientation). This load transfer also correlated to the maximum load achieved (**Figure 4.10**). Similar to stiffness, the maximum load increased as the orientation and basis weight parameter increased. Thus the initial microstructure surrounding the bond affected the load even after the initial low displacement and, indeed, determined how the bond sustained load.

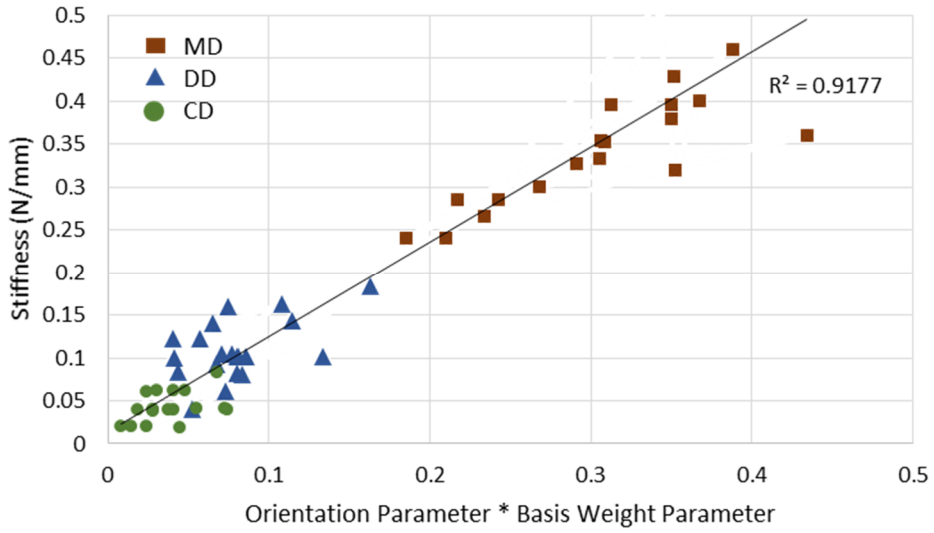

Figure 4.9: Orientation parameter & basis weight parameter versus stiffness.

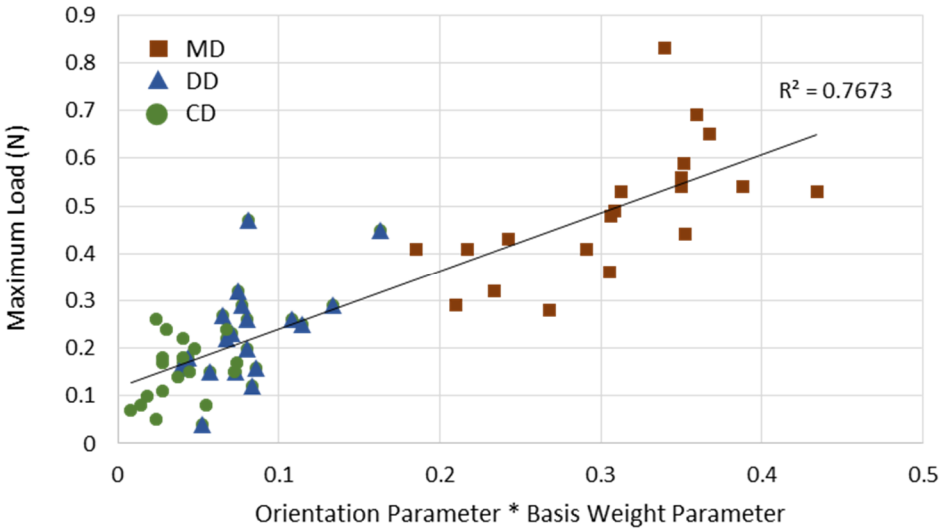

Figure 4.10: Orientation parameter & basis weight parameter versus maximum load.

By using these two parameters, fiber orientation, and basis weight, one can systematically reduce the intrinsic variation in the force response. **Figure 4.9** and **Figure 4.10** indicate that measuring the fiber orientation and basis weight around a bond provide a correlation to the mechanical properties. Discerning the influence of processing parameters on the mechanical properties of a bond would be extremely difficult without

accounting for variations in fiber orientation or basis weight. Similarly, modeling a nonwoven system without accounting for the bond deformations and the structural variations would lead to inaccurate predictions.

Chapter 5: Conclusions and Future Work

This research shows conclusive results for a novel method to analyze point-bonded nonwoven fabrics. It has quantitatively shown that the microstructure surrounding a bond is correlated to the mechanics and failure mode of that bond. The amount of fibers, as well as the direction of those fibers, allow the load to be transmitted through a bond and distribute the load across the system.

The bond cannot reach a yield point unless a significant number of fibers transfer a load into the bond. Consequently, bond yielding only occurs when the surrounding microstructure has enough fibers and high degrees of fiber orientation, typically MD. Individual fiber failure was observed throughout all tests, but it played a more significant role for bonds within the lower fiber orientation directions, DD and CD.

References

1. *The future of global nonwovens markets to 2020*. 2015: Smithers Pira Market Intelligence.
2. Backer, S. and D.R. Petterson, *Some principles of nonwoven fabrics 1.* Textile Research Journal, 1960. **30**(9): p. 704-711.
3. Chester, S.O., A. Witarsa, S. Streich, H. Hartl, H. Siebner, D. Kong and D.D. Newkirk, *Extensible nonwoven fabric*. 2015, Google Patents.
4. Choudhury, A.K.R., *Textile preparation and dyeing*. 2006: Science Publishers.
5. Russell, S.J., *Handbook of nonwovens*. 2006: Woodhead Publishing.
6. Albrecht, W., H. Fuchs and W. Kittelmann, *Nonwoven fabrics: raw materials, manufacture, applications, characteristics, testing processes*. 2006: John Wiley & Sons.
7. Kim, H.S., B. Pourdeyhimi, A.S. Abhiraman and P. Desai, *Effect of bonding temperature on Load-deformation structural changes in point-bonded nonwoven fabrics.* Textile Research Journal, 2002. **72**(7): p. 645-653.
8. Oxman, N., *Material-based design computation*. 2010, Massachusetts Institute of Technology.
9. Riedel, J.E. and I. Association of the Nonwoven Fabrics, *Principles of nonwovens*. 1993, Cary, N.C: INDA, Association of the Nonwoven Fabrics Industry.
10. Hearle, J.W.S., *The structural mechanics of fibers.* Journal of Polymer Science Part C: Polymer Symposia, 1967. **20**(1): p. 215-251.

11. Samuels, R.J., *Spherulite structure, deformation morphology, and mechanical properties of isotactic polypropylene fibers.* Journal of Polymer Science Part C: Polymer Symposia, 1967. **20**(1): p. 253-284.

12. Spruiell, J.E. and J.L. White, *Structure development during polymer processing: Studies of the melt spinning of polyethylene and polypropylene fibers.* Polymer Engineering & Science, 1975. **15**(9): p. 660-667.

13. Osta, A.R., C.R. Picu, A. King, O. Isele, R. Hamm and A. Dreher, *Effect of polypropylene fiber processing conditions on fiber mechanical behavior.* Polymer International, 2014. **63**(10): p. 1816-1823.

14. Nielsen, A.S., D.N. Batchelder and R. Pyrz, *Estimation of crystallinity of isotactic polypropylene using Raman spectroscopy.* Polymer, 2002. **43**(9): p. 2671-2676.

15. Zahn, H., P. Kusch, D. Müller-Schulte, D. Nissen and V. Rossbach, *The impact of natural fiber science on manmade fiber technology 1.* Textile Research Journal, 1973. **43**(10): p. 601-606.

16. Dasdemir, M., B. Maze, N. Anantharamaiah and B. Pourdeyhimi, *Influence of polymer type, composition, and interface on the structural and mechanical properties of core/sheath type bicomponent nonwoven fibers.* Journal of Materials Science, 2012. **47**(16): p. 5955-5969.

17. Mukhopadhyay, S., *Bi-component and bi-constituent spinning of synthetic polymer fibres.* Advances in Filament Yarn Spinning of Textiles and Polymers, 2014: p. 113.

18. El-Shiekh, A., J.F. Bogdan and R.K. Gupta, *The mechanics of bicomponent fibers: part I : theoretical analysis.* Textile Research Journal, 1971. **41**(4): p. 281-297.

19. El-Shiekh, A., J.F. Bogdan and R.K. Gupta, *The mechanics of bicomponent fibers: part II: experimental investigation.* Textile Research Journal, 1971. **41**(11): p. 916-922.

20. Perret, E., F.A. Reifler, R. Hufenus, O. Bunk and M. Heuberger, *Modified crystallization in PET/PPS bicomponent fibers revealed by small-angle and wide-angle X-ray scattering.* Macromolecules, 2012. **46**(2): p. 440-448.

21. Michielsen, S., B. Pourdeyhimi and P. Desai, *Review of thermally point-bonded nonwovens: Materials, processes, and properties.* Journal of Applied Polymer Science, 2006. **99**(5): p. 2489-2496.

22. Kim, Y.H. and R.P. Wool, *A theory of healing at a polymer-polymer interface.* Macromolecules, 1983. **16**(7): p. 1115-1120.

23. Wool, R.P., *Polymer interfaces: structure and strength*. 1995: Hanser.

24. Wool, R., B.L. Yuan and O. McGarel, *Welding of polymer interfaces.* Polymer Engineering & Science, 1989. **29**(19): p. 1340-1367.

25. Dharmadhikary, R.K., T. Gilmore, H. Davis and S. Batra, *Thermal bonding of nonwoven fabrics.* Textile Progress, 1995. **26**(2): p. 1-37.

26. Kim, H.S., B. Pourdeyhimi, P. Desai and A.S. Abhiraman, *Anisotropy in the mechanical properties of thermally spot-bonded nonwovens: experimental observations.* Textile Research Journal, 2001. **71**(11): p. 965-976.

27. Bhat, G.S., P.K. Jangala and J.E. Spruiell, *Thermal bonding of polypropylene nonwovens: effect of bonding variables on the structure and properties of the fabrics.* Journal of Applied Polymer Science, 2004. **92**(6): p. 3593-3600.

28. Wei, K., T. Vigo and B. Goswami, *Structure–property relationships of thermally bonded polypropylene nonwovens.* Journal of Applied Polymer Science, 1985. **30**(4): p. 1523-1534.

29. Wang, X. and S. Michielsen, *Morphology gradients in thermally point-bonded polypropylene nonwovens.* Textile Research Journal, 2001. **71**(6): p. 475-480.

30. Wang, X. and S. Michielsen, *Isotactic polypropylene morphology–Raman spectra correlations.* Journal of Applied Polymer Science, 2001. **82**(6): p. 1330-1338.

31. De Baez, M.A., P. Hendra and M. Judkins, *The Raman spectra of oriented isotactic polypropylene.* Spectrochimica Acta Part A: Molecular and Biomolecular Spectroscopy, 1995. **51**(12): p. 2117-2124.

32. Chand, S., G.S. Bhat, J.E. Spruiell and S. Malkan, *Structure and properties of polypropylene fibers during thermal bonding.* Thermochimica acta, 2001. **367**: p. 155-160.

33. Farukh, F., D. Emrah, A. Memiş, P. Behnam and V.S. Vadim, *Strength of fibres in low-density thermally bonded nonwovens: An experimental investigation.* Journal of Physics: Conference Series, 2012. **382**(1): p. 012018.

34. Chidambaram, A., *Fundamentals of fiber bonding in thermally point-bonded nonwovens*. 1999, North Carolina State University: Ann Arbor. p. 107-107 p.

35. Farukh, F., E. Demirci, B. Sabuncuoglu, M. Acar, B. Pourdeyhimi and V.V. Silberschmidt, *Mechanical analysis of bi-component-fibre nonwovens: Finite-element strategy.* Composites Part B: Engineering, 2015. **68**: p. 327-335.

36. Demirci, E., M. Acar, B. Pourdeyhimi and V.V. Silberschmidt, *Finite element modelling of thermally bonded bicomponent fibre nonwovens: Tensile behaviour.* Computational Materials Science, 2011. **50**(4): p. 1286-1291.

37. E. Demirci, M.A., B. Pourdeyhimi, V. V. Silberschmidt, *Dynamic response of thermally bonded bicomponent fibre nonwovens.* Applied Mechanics and Materials, 2011. **70**: p. 405-409.

38. Rawal, A., S. Lomov and I. Verpoest, *An environmental scanning electron microscope study of a through-air bonded structure under tensile loading.* Journal of the Textile Institute, 2008. **99**(3): p. 235-241.

39. Rawal, A. and S.K. Agrahari, *Pore size characteristics of nonwoven structures under uniaxial tensile loading.* Journal of Materials Science, 2011. **46**(13): p. 4487-4493.

40. Kim, H.S., A. Deshpande, B. Pourdeyhimi, A.S. Abhiraman and P. Desai, *Characterizing structural changes in point-bonded nonwoven fabrics during load-deformation experiments.* Textile Research Journal, 2001. **71**(2): p. 157-164.

41. Hou, X., M. Acar and V. Silberschmidt, *Non-uniformity of deformation in low-density thermally point bonded non-woven material: effect of microstructure.* Journal of Materials Science, 2011. **46**(2): p. 307-315.

42. Veerabadran, R., H.A. Davis, S.K. Batra and A.C. Bullerwell, *Devices for on-line assessment of nonwovens' basis weights and structures.* Textile Research Journal, 1996. **66**(4): p. 257-264.

43. Pourdeyhimi, B. and H.S. Kim, *Measuring fiber orientation in nonwovens: the hough transform.* Textile Research Journal, 2002. **72**(9): p. 803-809.

44. Demirci, E., M. Acar, B. Pourdeyhimi and V.V. Silberschmidt, *Computation of mechanical anisotropy in thermally bonded bicomponent fibre nonwovens.* Computational Materials Science, 2012. **52**(1): p. 157-163.

45. Rawal, A., A. Priyadarshi, N. Kumar, S.V. Lomov and I. Verpoest, *Tensile behaviour of nonwoven structures: comparison with experimental results.* Journal of Materials Science, 2010. **45**(24): p. 6643-6652.

46. Rawal, A., A. Priyadarshi, S.V. Lomov, I. Verpoest and J. Vankerrebrouck, *Tensile behaviour of thermally bonded nonwoven structures: model description.* Journal of Materials Science, 2010. **45**(9): p. 2274-2284.

47. Rawal, A., P.K. Mishra and H. Saraswat, *Modeling the compression-induced morphological behavior of nonwoven materials.* Journal of Materials Science, 2012. **47**(5): p. 2365-2374.

48. Amiot, M., M. Lewandowski, P. Leite, M. Thomas and A. Perwuelz, *An evaluation of fiber orientation and organization in nonwoven fabrics by tensile, air permeability and compression measurements.* Journal of Materials Science, 2014. **49**(1): p. 52-61.

49. Hou, X., M. Acar and V.V. Silberschmidt, *Finite element simulation of low-density thermally bonded nonwoven materials: Effects of orientation distribution*

function and arrangement of bond points. Computational Materials Science, 2011. **50**(4): p. 1292-1298.

50. Sozumert, E., F. Farukh, E. Demirci, M. Acar, B. Pourdeyhimi and V.V. Silberschmidt, *Damage mechanisms of random fibrous networks.* Journal of Physics: Conference Series, 2015. **628**(1): p. 012093.

51. Farukh, F., E. Demirci, B. Sabuncuoğlu, M. Acar, B. Pourdeyhimi and V.V. Silberschmidt, *Characterisation and numerical modelling of complex deformation behaviour in thermally bonded nonwovens.* Computational Materials Science, 2013. **71**: p. 165-171.

52. Rezakhaniha, R., A. Agianniotis, J.T.C. Schrauwen, A. Griffa, D. Sage, C. Bouten, F. Van de Vosse, M. Unser and N. Stergiopulos, *Experimental investigation of collagen waviness and orientation in the arterial adventitia using confocal laser scanning microscopy.* Biomechanics and Modeling in Mechanobiology, 2012. **11**(3-4): p. 461-473.

53. Cox, H., *The elasticity and strength of paper and other fibrous materials.* British Journal of Applied Physics, 1952. **3**(3): p. 72.